SENSITIVITY OF ACTIVE VIBRATION CONTROL TO STRUCTURAL CHANGES AND MODEL REDUCTION

by

Zoran N. Martinovic

Dissertation submitted to the Faculty of the

Virginia Polytechnic Institute and State University

in partial fulfillment of the requirements for the degree of

Doctor of Philosophy

in

Aerospace Engineering

APPROVED:

Raphael T. Haftka, Chairman

William L. Hallauer, Jr.

Henry J. Kelley

Leonard Meirovitch

Eric R. Johnson

May, 1987

Blacksburg, Virginia

SENSITIVITY OF ACTIVE VIBRATION CONTROL TO STRUCTURAL CHANGES AND MODEL REDUCTION

by

Zoran N. Martinovic

Raphael T. Haftka, Chairman

Aerospace Engineering

(ABSTRACT)

The analytical study presented here is concerned with by two types of sensitivity of active vibration control of large space structures (LSS). The first one required for assessing robustness, is the sensitivity of the performance and stability of the control system to changes in structure and to model reduction. The second type is the sensitivity of the optimum design of the control system to changes in the structure. This sensitivity is of interest in assessing the need for integrated structure/control design.

Three direct rate feedback (DRF) control techniques are studied for a laboratory structure which has characteristics of LSS and then compared to standard linear quadratic (LQ) control. The baseline design of each control system is obtained first and then sensitivity analysis conducted.

An uncoupled DRF control law which minimized the sum of gains subject to requirements on performance was not robust to structural changes, and small changes in the structure caused notable increase in performance compared to that of the baseline design and therefore a potential gain from simultaneous structure/control design was indicated.

Two coupled DRF techniques are proposed. A Minimum Force DRF (MF-DRF) law minimized maximum force of any actuator, while a Linear Quadratic DRF (LQ-DRF) law minimized the standard quadratic performance index for initial conditions in the shape of the first six natural modes. Both techniques guaranteed system stability. The LQ control law was found to be only slightly better than the simpler MF-DRF law in terms of the quadratic performance index and poorer than the LQ-DRF law. However the LQ control requires model reduction and was found to be sensitive to errors in that process. For example, the LQ design lost its stability when the structure was modified by adding a non-structural mass to it.

A separate experimental study was conducted simultaneously with this study to verify theoretical results. Good agreement was found between analytical results and experimental measurements for the investigated control techniques.

Acknowledgements

I wish to express my sincere gratitude to , my advisor, for his constant guidance and assistance throughout the course of my graduate work. His unwavering support, sometimes under difficult conditions and stages of my study, proved to be crucial.

I am indebted to Dr. William L. Hallauer Jr. for his close attention and timely help during the past years. His guidance of parallel experimental study enhanced my physical understanding of the problem at hand.

All the experimental results published here were obtained by

, to whom I extend my appreciation.

I would like to thank the members of my committee: Dr. Leonard Meirovitch, Dr. Henry J. Kelley, and Dr. Eric R. Johnson.

This research was supported by the National Aeronautics and Space Administration Grant NAG-1-224 and I gratefully acknowledge this financial support.

The enthusiastic and inspiring conversations with Dr. Andre Preumont are greatly appreciated. I am also grateful to Dr. Rajiv Thareja, Dr. Junjiro Onoda, Dr. Stanoje P. Bingulac, and Dr. Zeen C. Kim for their help with computer support. I acknowledge the assistance of my fellow graduate students

and of Femoyer Lounge.

Table of Contents

List of Illustrations

List of Tables

Chapter 1

Introduction

In the past ten years there has been growing interest in using active control in construction and operation of large structures in space (LSS) [1]. Because of the high cost of lifting mass to orbit LSS will be light weight and hence be quite flexible and have small inherent damping. Also, shape control requirements can be very severe for some LSS, such as large space antennas [2]. The combination of light weight and required shape accuracy present new and difficult control challenges addressed in many recent works.

In general there are three different types of active control of LSS: attitude control, static shape control, and active vibration suppression to satisfy precision pointing and alignment requirements. The present work is concerned with the active vibration control of LSS.

The dynamic behavior of flexible LSS is rigorously described by continuum theories expressed mathematically by partial differential equations of motion.

However, except for some simple cases, no closed-form solutions of the continuum equations of motion can be expected. Therefore, the structure is usually discretized in space by numerical procedures [3] such as the finite element method, and an approximate solution is obtained from finite-order model of the structure.

Many analytical studies of active vibration control are based on a linear quadratic (LQ) optimal control law [4]. However, this control strategy requires a controller which is the same order as the model of the structure. It is typically difficult to design, and impossible to implement a controller which is of the same order as the finite element model used to model a large space structure. Consequently, the control system is designed based on a reduced order model of the structure including the first few vibration modes which means further reduction (and approximation) of the dynamics of the structure for the control design purposes. The modal truncation of the structural model can result in a control system which destabilizes higher order residual modes, a phenomenon known as spillover instability [5]. For this reason there is interest in modifying the LQ design process to guarantee the stability of the unmodeled dynamics [6-8].

Even with a reduced model of the structure, the LQ control system design may be difficult to implement. Therefore some recent experimental studies simulating the control of large space structures have employed suboptimal but simple control laws [9-13]. A large group of control techniques consider direct output feedback control [9-10, 12-20], to achieve simpler implementation. Hale [21] attempts to maximize the allowable magnitude of an unknown but bounded dis-

turbance to the structure while explicitly satisfying specific input and output constraints thus allowing real physical constraints to drive the solution rather than vague quadratic penalties in an LQ cost function.

Besides guaranteeing global asymptotic stability, another desirable property of any control system is its ability to remain stable over a wide range of disturbances and modeling errors. The later quality may be defined by sensitivity of a control system to small changes in the system (or conversely the robustness). Of special interest in LSS control problem is sensitivity of closed-loop control system to small changes in the structure.

Therefore, a fundamental control design problem for large flexible space structures is designing low-order controllers for continuum (infinite-dimensional) structures in the presence of disturbances and modeling errors.

Two aspects of such sensitivity may then be identified. The first is the sensitivity of the performance and/or stability of the control system, which is usually associated with the robustness of the system. If the performance of closed-loop system in the face of uncertainties is acceptable then that system is said to possess performance robustness. If the control system remains stable in the face of uncertainties then the system is said to possess stability robustness.

Recently published literature on control system robustness is concerned primarily with the LQ control law formulation and measures of control robustness are expressed either in frequency-domain analysis or in time-domain analysis. The importance of robustness of multivariable control systems is discussed by Hoehne [22]. Singular value robustness measures are used in [23] to compare

performance and stability robustness properties of LQ based control design techniques in frequency-domain. A positivity concept is applied [6] to feedback controller design using positive real transfer function, and the minimum singular value of the return difference matrix was used to examine stability robustness of the closed loop plant in the presence of unmodeled modes. In [24] the stability robustness aspect is analyzed in the time-domain and a bound on the perturbation of an asymptotically stable linear system is obtained to maintain stability using Lyapunov matrix equation solution. Effects of errors in modal frequencies, damping, mode slopes, and moment of inertia on stability, time to null, and control requirements for decoupled control and LQ control are investigated in [25]. Sensitivity analysis approach is applied to directly calculate derivatives of the closed-loop performance with respect to given parameters for LQ control [26-28]. Junkins and Rew [29] emphasize an eigenstructure assignment method over the LQ methods. Their method seeks to maximize system robustness by minimizing the condition number of the closed loop modal matrix. Similarly, pole placement techniques and singular value robustness measures are used in Ref. [30]. A study of the sensitivity of a distributed structure to feedback controls designed on the basis of a discretized model was performed by Meirovitch and Norris [31].

Robustness was also investigated for output feedback control [32,33] and for direct rate feedback [15] in which the sensors and actuators are colocated, and for the independent modal-space control method [34] in which modal feedback forces are designed for each controlled mode independently of the other.

The second aspect of sensitivity is the sensitivity of the optimum design of the control system to changes in the structure, which is important in the assessment of the need for combined control/structural design. Recently, there has been considerable interest in simultaneous design of the structure and the control so as to produce a truly optimum configuration [35-44]. Before one embarks on such an undertaking, it is important to determine that there is a synergistic effect in designing a structure and control symultaneously. Several works [43, 45-46] approached the problem indirectly, by showing that the performance of the control system may be enhanced by optimizing the structure to improve a structural performance index such as the overall stiffness or a vibration frequency. Behavior sensitivities for control augmented structure with direct output feedback were studied in [16]. References [47-48] approach the question of the possible synergistic effect more directly by showing that minor structural modifications can have a large effect on the control system performance. They also demonstrated how the magnitude of the synergistic effect can be predicted from a sensitivity analysis of the control performance.

The present work has three objectives. The first is to study the two aspects of the sensitivity of a controlled structure to changes in the structure: the sensitivity of the performance and stability, and the sensitivity of the optimum design of the control system.

The second objective is to develop simple and robust control laws suitable for laboratory implementation and compare their performance to the LQ design.

The third goal is to compare accuracy of theoretical results obtained for all considered control systems against experimental results obtained for a laboratory structure built to have some characteristics of LSS. However, performance of experimental measurements was not part of this study.

Sensitivity analysis of optimized systems is used to predict the changes required in the control system to take full advantage of the structural modifications, and the ensuing change in performance. Sensitivity calculations are carried out analytically and validated experimentally for a flexible cruciform beam supported by cables. The potential synergistic effect is established when small structural modifications can produce large reductions in the control strength required to achieve a desired level of active damping.

Control system modeling and calculation of eigenvalues and their derivatives with respect to the problem parameters is presented in Chapter 2. Structural model reduction required for design of low-order LQ controller is also discussed in the same chapter. The theoretical development of each control technique is given in Chapter 3: the standard LQ control, as well as two new proposed direct rate feedback control laws. The effects of model reduction are discussed as well as analytical design optimization and sensitivity derivations. Chapter 4 compares results obtained for baseline designs of all control systems for the beam structure. The effects of small structural changes and model reduction on control system designs and performance are presented in Chapter 5. A summary and conclusions are given in Chapter 6.

Chapter 2

Analytical Model

2.1 Control System Modeling

The equations of motion for a structure with n_n degrees of freedom (DOF) and controlled by n_c actuators are

$$\mathbf{M}_s\ddot{\mathbf{q}}(t) + \mathbf{C}_s\dot{\mathbf{q}}(t) + \mathbf{K}_s\mathbf{q}(t) = \mathbf{U}_s\mathbf{u}(t). \tag{2.1}$$

where $\mathbf{M}_s$, $\mathbf{C}_s$, and $\mathbf{K}_s$ are the $n_n x n_n$ mass, inherent viscous damping, and stiffness matrices respectively. We assume that $\mathbf{C}_s$ does not couple the undamped modes of vibration. $\mathbf{q}$ is an $n_n x 1$ vector of physical or generalized displacement components, and $\mathbf{U}_s$ is an $n_n x n_c$ applied load distribution matrix relating the $n_c x 1$ control input vector $\mathbf{u}$ to the structural DOF.

We introduce the $2n_n x 1$ state vector $\mathbf{x}$:

$$\mathbf{x}(t) = \begin{Bmatrix} \dot{\mathbf{q}}(t) \\ \mathbf{q}(t) \end{Bmatrix} \tag{2.2}$$

and assume uncertainties and random disturbances in the system by introducing state excitation noise $\mathbf{w}_1$. Then, Eq. (2.1) can be written in state vector form as

$$\dot{\mathbf{x}}(t) = \mathbf{A}\,\mathbf{x}(t) + \mathbf{B}\,\mathbf{u}(t) + \mathbf{w}_1(t) \tag{2.3}$$

The $2n_m x 2n_m$ system matrix **A** is

$$\mathbf{A} = \begin{bmatrix} -\mathbf{M}_s^{-1}\mathbf{C}_s & -\mathbf{M}_s^{-1}\mathbf{K}_s \\ \mathbf{I} & \mathbf{0} \end{bmatrix} \tag{2.4}$$

where matrices **I** and **0** are identity and zero matrices of order n_m and the $2n_m x n_c$ control matrix **B** is

$$\mathbf{B} = \begin{bmatrix} \mathbf{M}_s^{-1}\mathbf{U}_s \\ \mathbf{0} \end{bmatrix} \tag{2.5}$$

where **0** is a zero matrix of order $n_m x n_c$. We assume that the system is time invariant, that is **A** and **B** are constant.

To prevent numerical ill-conditioning it is desirable that $\mathbf{q}$ and $\dot{\mathbf{q}}$ components of $\mathbf{x}$ be of the same order of magnitude. This can be achieved by using the reciprocal of a typical frequency as the time unit. In the present work the time unit employed was 10^{-2} second (cs).

It is either impossible or not desirable, for engineering reasons, to measure all the structural state variables. Therefore, only n_s states are measured by sen-

sors and these are represented by a vector **y** which is subject to contamination by a vector $\mathbf{w}_2$ of observation or measurement noise

$$\mathbf{y}(t) = \mathbf{C}\mathbf{x}(t) + \mathbf{w}_2(t) \tag{2.6}$$

where **C** is the $n_s x 2n_m$ observation matrix.

The control law is assumed to be linear, and if all structural state variables are measured and fed back then the control law is given as

$$\mathbf{u}(t) = -\mathbf{F}\mathbf{x}(t). \tag{2.7}$$

with a gain matrix **F** ($n_c x 2n_m$). If only a few state variables are measurable, and the same form of control is used, then a state estimator (observer, filter) must be used to estimate **x** on the basis of sensor measurements and the analytical model. An estimate $\hat{\mathbf{x}}$ of **x** is often obtained from the vector of output measurements **y** by using an observer which solves

$$\dot{\hat{\mathbf{x}}}(t) = \mathbf{A}\hat{\mathbf{x}}(t) + \mathbf{B}\mathbf{u}(t) + \mathbf{K}[\mathbf{y}(t) - \mathbf{C}\hat{\mathbf{x}}(t)] \tag{2.8}$$

where filter gain matrix is the **K** ($2n_m x n_s$). Eq. (2.7) is replaced by

$$\mathbf{u}(t) = -\mathbf{F}\hat{\mathbf{x}}(t) \tag{2.9}$$

An alternative is to use output feedback which uses only the vector **y** so that **u** is given as

$$\mathbf{u}(t) = -\mathbf{D}\mathbf{y}(t) \tag{2.10}$$

where **D** is an ($n_c x n_s$) gain matrix.

2.2 Calculation of Eigenvalues and Their Derivatives

Another form of Eq. (2.1) which will be used in the output feedback analysis is:

$$\mathbf{M}^*\dot{\mathbf{x}}(t) + \mathbf{K}^*\mathbf{x}(t) = \mathbf{0} \tag{2.11}$$

where

$$\mathbf{M}^* = \begin{bmatrix} \mathbf{0} & \mathbf{M}_s \\ \mathbf{M}_s & \mathbf{C}_s + \mathbf{U}_s\mathbf{D}\mathbf{C}_v \end{bmatrix} \tag{2.12}$$

$$\mathbf{K}^* = \begin{bmatrix} -\mathbf{M}_s & \mathbf{0} \\ \mathbf{0} & \mathbf{K}_s \end{bmatrix} \tag{2.13}$$

and the observation matrix in Eq. (2.6) is

$$\mathbf{C} = [\mathbf{C}_v \quad \mathbf{0}] \tag{2.14}$$

where $\mathbf{C}_v$ is the $n_s x n_n$ partition of the observation matrix and output is

$$\mathbf{y}(t) = \mathbf{C}_v\dot{\mathbf{q}}(t) \tag{2.15}$$

Assuming a solution of Eq. (2.11) of the form

$$\mathbf{x}(t) = e^{\mu t}\boldsymbol{\varphi} \tag{2.16}$$

the associated eigenvalue problem becomes

$$(\mu\mathbf{M}^{*} + \mathbf{K}^{*})\boldsymbol{\varphi} = \mathbf{0} \tag{2.17}$$

For small or moderate values of damping the solution of Eq. (2.17) yields n_n complex conjugate eigenvalue pairs

$$\mu_r = \sigma_r \pm j\omega_r \qquad r = 1,\ldots, n_n \tag{2.18}$$

The damping factor of the r-th mode is defined as

$$\zeta_r = \frac{-\sigma_r}{\sqrt{\sigma_r^2 + \omega_r^2}} \tag{2.19}$$

The real and imaginary parts may be written in terms of a nominal frequency ω_{0r} and ζ_r as

$$\sigma_r = -\zeta_r\omega_{0r}, \qquad \omega_r = \omega_{0r}\sqrt{1 - \zeta_r^2} \tag{2.20}$$

For the design of the structure and control system, we require the derivatives of the eigenvalues μ_r with respect to design parameters s_i. These derivatives may be calculated by finite difference, but this can become quite expensive. Therefore, analytical derivatives have been derived (in a manner similar to that of Ref. 49) and employed.

Differentiating Eq. (2.11) with respect to a design variable p_r for the r-th eigenpair, one obtains

$$(\mu_r \mathbf{M}^* + \mathbf{K}^*)\frac{\partial \boldsymbol{\varphi}_r}{\partial s_i} + \frac{\partial \mu_r}{\partial s_i}\mathbf{M}^*\boldsymbol{\varphi}_r + \left(\mu_r \frac{\partial \mathbf{M}^*}{\partial s_i} + \frac{\partial \mathbf{K}^*}{\partial s_i}\right)\boldsymbol{\varphi}_r = \mathbf{0} \tag{2.21}$$

After premultiplying Eq. (2.21) by the transpose of the r-th eigenvector and rearranging terms, one obtains

$$\frac{\partial \mu_r}{\partial s_i} = \frac{-\boldsymbol{\varphi}_r^T\left(\mu_r \frac{\partial \mathbf{M}^*}{\partial s_i} + \frac{\partial \mathbf{K}^*}{\partial s_i}\right)\boldsymbol{\varphi}_r}{\boldsymbol{\varphi}_r^T \mathbf{M}^* \boldsymbol{\varphi}_r} \tag{2.22}$$

Equation (2.22) can also be expressed in the following form,

$$\frac{\partial \mu_r}{\partial s_i} = \frac{\partial \sigma_r}{\partial s_i} \pm j\frac{\partial \omega_r}{\partial s_i} \tag{2.23}$$

The derivative of the damping ratio for the r-th mode is obtained by differentiating Eq. (2.19) with respect to the design variable s_i,

$$\frac{\partial \zeta_r}{\partial s_i} = \frac{\omega_r\left(\sigma_r \frac{\partial \omega_r}{\partial s_i} - \omega_r \frac{\partial \sigma_r}{\partial s_i}\right)}{(\sigma_r^2 + \omega_r^2)^{3/2}} \tag{2.24}$$

2.3 Structural Model Reduction

The number n_n of DOFs of the analytical model may have to be reduced to n_R to meet the physical limitations of the control hardware. A model reduction scheme [50] based on the first n_R undamped modes of the system is used. However, the reduced vector of degrees of freedom $\mathbf{q}_R$ is not the modal amplitudes, but a subset of degrees of freedom in $\mathbf{q}$. The reduced matrices needed for obtaining reduced system and control matrices $\mathbf{A}_R$ and $\mathbf{B}_R$ are given as

$$\mathbf{M}_{sR}^{-1}\mathbf{C}_{sR} = \mathbf{\Phi}_R\,[diag(2\zeta_i\omega_i)]_R\,\mathbf{\Phi}_R^{-1} \tag{2.25}$$

$$\mathbf{M}_{sR}^{-1}\mathbf{K}_{sR} = \mathbf{\Phi}_R\,[diag(\omega_i^2)]_R\,\mathbf{\Phi}_R^{-1} \tag{2.26}$$

$$\mathbf{M}_{sR}^{-1}\mathbf{U}_{sR} = \mathbf{\Phi}_R\,[diag(\mathrm{M}_i^{-1})]_R\,\mathbf{\Phi}_R^{T}\mathbf{U}_{sR} \tag{2.27}$$

$\mathbf{\Phi}_R$ is the $n_R x n_R$ partition of the full modal matrix $\mathbf{\Phi}$ containing only DOFs and modes to be retained in the reduced model. $\mathbf{\Phi}$ is obtained from

$$\mathbf{M}_s\ddot{\mathbf{q}}(t) + \mathbf{K}_s\mathbf{q}(t) = \mathbf{0} \tag{2.28}$$

M_i, ζ_i , and ω_i are respectively the modal masses, inherent damping ratios and undamped natural frequencies ($\mathbf{C}_s = 0$) of the retained modes. This model re-

duction preserves exactly the dynamic response of the retained DOFs in the retained modes. The details of the model reduction are presented in Appendix A.

Chapter 3

Control System Design

3.1 Linear Quadratic Optimal Control

3.1.1 Linear Quadratic Regulator

The commonly used deterministic (i.e. $\mathbf{w}_1 = \mathbf{0}$) linear quadratic regulator (LQR) has performance index [51] of the form

$$J = \int_0^\infty [\mathbf{x}(t)^T \mathbf{Q}\mathbf{x}(t) + \mathbf{u}(t)^T \mathbf{R}\mathbf{u}(t)]dt \tag{3.1}$$

where **Q** and **R** are non-negative definite state weighting matrix ($2n_n x 2n_n$) and positive definite control weighting matrix ($n_c x n_c$) respectively. By proper selection

of the elements of these matrices, it is possible to control the magnitudes of the actuator forces and the rate of decay of vibration amplitudes.

The selection of weighting matrices **Q** and **R** represents a compromise between fast damping of the state **x** promoted by increasing **Q** with respect to **R**, and small control forces **u** promoted by increasing **R** with respect to **Q**. With linear control defined by Eq. (2.7), the optimum gain matrix **F** ($n_c x 2n_n$) required for the control input is given as

$$\mathbf{F} = \mathbf{R}^{-1}\mathbf{B}^T\mathbf{S}_r, \tag{3.2}$$

where for steady-state control $\mathbf{S}_r$ is found by solving an algebraic matrix Riccati equation

$$\mathbf{A}^T\mathbf{S}_r + \mathbf{S}_r\mathbf{A} - \mathbf{S}_r\mathbf{B}\,\mathbf{R}^{-1}\mathbf{B}^T\mathbf{S}_r + \mathbf{Q} = \mathbf{0}, \tag{3.3}$$

The LQR law is designed using the assumption that there is no uncertainty (i.e. $\mathbf{w}_1 = 0$ and $\mathbf{w}_2 = 0$) in the system. That is, there are no control hardware errors, no unknown structural disturbances, that we can measure exactly all state variables ($\mathbf{q}$ and $\dot{\mathbf{q}}$) and output variables, and that the structural parameters are known exactly.

The optimum value of the performance index for a given vector $\mathbf{x}_0$ of initial conditions is then

$$J_{\min} = \mathbf{x}_0^T\mathbf{S}_r\mathbf{x}_0 \tag{3.4}$$

In the present study we choose initial conditions in the shape of one of the first six open-loop mode shapes (φ) normalized so that the maximum element of each equals one inch

$$\mathbf{x}_0 = \begin{Bmatrix} \mathbf{0} \\ \boldsymbol{\varphi} \end{Bmatrix} \tag{3.5}$$

3.1.2 Linear Quadratic Gaussian Control

If uncertainties are modeled in the system, then $\mathbf{w}_1 \neq 0$, $\mathbf{w}_2 \neq 0$ and the output $\mathbf{y}$ from the system is defined in Eq. (2.6). Both state excitation noise ($\mathbf{w}_1$) and observation noise ($\mathbf{w}_2$) are assumed to be uncorrelated Gaussian white noise processes with zero mean and intensities (covariance matrices) $\mathbf{V}_1$ and $\mathbf{V}_2$. The estimate $\hat{\mathbf{x}}$ of structural state variables is obtained by solving Eq. (2.8). In the present study a Kalman filter is used as the observer, and then the filter gain matrix $\mathbf{K}$ ($2n_r \times n_s$) in Eq. (2.8) is given as

$$\mathbf{K} = \mathbf{S}_f \mathbf{C}^T \mathbf{V}_2^{-1} \tag{3.6}$$

where $\mathbf{S}_f$ is found by solving another Riccati equation

$$(\mathbf{A} + \alpha\mathbf{I})\,\mathbf{S}_f + \mathbf{S}_f(\mathbf{A} + \alpha\mathbf{I})^T - \mathbf{S}_f \mathbf{C}^T \mathbf{V}_2^{-1} \mathbf{C}\, \mathbf{S}_f + \mathbf{V}_1 = \mathbf{0}, \tag{3.7}$$

which depends on assumed system and measurement noise intensities, $\mathbf{V}_1$ and $\mathbf{V}_2$ respectively. The positive scalar α represents a prescribed degree of filter stability

[52,53] (also see Appendix B.), that is the real part of each filter pole is required to be more negative than $-\alpha$. The optimal input command **u** is defined then in Eq. (2.9). We refer to the combination of Kalman filter and regulator as the controller.

The optimal filter provides a compromise between the speed of state reconstruction and insensitivity to observation noise. The filter should be sufficiently fast to reconstruct the regulator state (i.e. filter poles should have more negative real parts than regulator poles), yet slow enough to be insensitive to high frequency excitation and measurement noise (i.e. filter poles should not be too negative). This is achieved by adjusting V_1, V_2, and α. By reducing V_2 for instance, we improve the speed of state reconstruction (shifting the observer poles further left in the complex plane), since lower priority is given to filtering the observation noise. A similar effect can be achieved by increasing V_1 or α .

We assume that elements of the noise vectors are uncorrelated, that is V_1 and V_2 are diagonal matrices. In the present study the V_1 matrix was chosen based on an estimate of system noise, while the V_2 matrix and α were selected to achieve a desired location of the filter poles and separation of the filter poles from the regulator poles in the complex plane.

The combined system of LQR and Kalman filter is denoted Linear Quadratic Gaussian (LQG) control.

3.1.3 Calculation of Performance for LQG Control

For assessing the loss of performance associated with the use of an observer rather than measuring the entire state vector, we disregard the noise and use the quadratic performance index (Eq. 3.1) with $\mathbf{w}_1 = \mathbf{0}$ and $\mathbf{w}_2 = \mathbf{0}$. The LQG control system can be described with an augmented state vector $\bar{\mathbf{x}}$ of dimension $4n_n$

$$\dot{\bar{\mathbf{x}}}(t) = \bar{\mathbf{A}}\,\bar{\mathbf{x}}(t) \tag{3.8}$$

where

$$\bar{\mathbf{A}} = \begin{bmatrix} \mathbf{A} - \mathbf{BF} & \mathbf{BF} \\ \mathbf{0} & \mathbf{A} - \mathbf{KC} \end{bmatrix} \tag{3.9}$$

and the augmented state vector is

$$\bar{\mathbf{x}}(t) = \begin{Bmatrix} \mathbf{x}(t) \\ \mathbf{e}(t) \end{Bmatrix} \tag{3.10}$$

where the state reconstruction error vector of order $2n_n$ is

$$\mathbf{e}(t) = \mathbf{x}(t) - \hat{\mathbf{x}}(t) \tag{3.11}$$

The optimal value of the performance index Eq. (3.1) is given (see Appendix D) as

$$J = \int_0^\infty [\bar{\mathbf{x}}(t)^T \bar{\mathbf{Q}} \bar{\mathbf{x}}(t)]dt \tag{3.12}$$

where

$$\overline{\mathbf{Q}} = \begin{bmatrix} \mathbf{Q} + \mathbf{F}^T\mathbf{R}\mathbf{F} & -\mathbf{F}^T\mathbf{R}\mathbf{F} \\ -\mathbf{F}^T\mathbf{R}\mathbf{F} & \mathbf{F}^T\mathbf{R}\mathbf{F} \end{bmatrix} \tag{3.13}$$

or

$$J_{\min} = \overline{\mathbf{x}}_0^T \overline{\mathbf{P}}\, \overline{\mathbf{x}}_0 \tag{3.14}$$

where the $4n_n x 4n_n$ matrix $\overline{\mathbf{P}}$ is the solution of the Lyapunov equation

$$\overline{\mathbf{A}}^T \overline{\mathbf{P}} + \overline{\mathbf{P}}\,\overline{\mathbf{A}} + \overline{\mathbf{Q}} = \mathbf{0} \tag{3.15}$$

We assume that the observer initial state estimate is $\hat{\mathbf{x}}_0 = \mathbf{0}$ and therefore the augmented initial state is

$$\overline{\mathbf{x}}_0 = \begin{Bmatrix} \mathbf{x}_0 \\ \mathbf{x}_0 \end{Bmatrix} \tag{3.16}$$

3.1.4 Effect of Controller using Reduced Order Model

To investigate the effect of model reduction, we analyze a full-order model of the structure connected to a controller designed for the reduced model. The combined structure/controller is a linear system of order $2n_n + 2n_R$

$$\dot{\mathbf{x}}_E(t) = \mathbf{A}_E\, \mathbf{x}_E(t) \tag{3.17}$$

where

$$\mathbf{x}_E(t) = \begin{Bmatrix} \mathbf{x}(t) \\ \hat{\mathbf{x}}_R(t) \end{Bmatrix} \tag{3.18}$$

and

$$\mathbf{A}_E = \begin{bmatrix} \mathbf{A} & -\mathbf{B}\mathbf{F}_R \\ \mathbf{K}_R\mathbf{C} & \mathbf{A}_R - \mathbf{K}_R\mathbf{C}_R - \mathbf{B}_R\mathbf{F}_R \end{bmatrix} \tag{3.19}$$

where $\mathbf{A}_R$, $\mathbf{B}_R$, $\mathbf{C}_R$, $\mathbf{F}_R$, and $\mathbf{K}_R$ are reduced forms of the **A**, **B**, **C**, **F** , and **K** matrices.

The quadratic performance index for reduced order control system can be evaluated as

$$J = \mathbf{x}_{E0}^T \mathbf{P}_E \mathbf{x}_{E0} \tag{3.20}$$

where the matrix $\mathbf{P}_E$ of order $2n_n + 2n_R$ is the solution of the Lyapunov equation

$$\mathbf{A}_E^T \mathbf{P}_E + \mathbf{P}_E \mathbf{A}_E + \mathbf{Q}_E = \mathbf{0} \tag{3.21}$$

with

$$\mathbf{Q}_E = \begin{bmatrix} \mathbf{Q} & \mathbf{0} \\ \mathbf{0} & \mathbf{F}_R^T \mathbf{R} \mathbf{F}_R \end{bmatrix} \tag{3.22}$$

We assume that the observer initial state estimate is $\hat{\mathbf{x}}_0 = \mathbf{0}$ and therefore the augmented initial state is

$$\mathbf{x}_{E0} = \begin{Bmatrix} \mathbf{x}_0 \\ \mathbf{0} \end{Bmatrix} \tag{3.23}$$

3.2 Direct Rate Feedback Optimized Control

3.2.1 Formulation of Design Problem

Direct rate feedback control (DRF) is a special case of direct output feedback control. Active vibration damping is effected by pairs of colocated velocity sensors and force actuators. The number of control pairs (n_c) is typically much smaller than the order of **x**, and only a vector **y** of n_c velocity elements $\dot{q}_j$ of the state vector is fed back in the closed loop, and is given by Eq. (2.10). The number of actuators and sensors is the same, so $n_s = n_c$. System stability is guaranteed if the active damping matrix **D** ($n_c x n_c$) is positive definite because this form of active damping can only dissipate energy [9-10, 17-18].

Two designs of DRF are considered here: uncoupled DRF, and coupled DRF. Several performance indices are investigated in order to select the best candidate for the further study. In all cases the control system is designed to achieve a required stability margin while minimizing a measure of the magnitude of the control gains or the elements of the matrix **D**.

3.2.2 Performance Indices for DRF Control

For uncoupled direct rate feedback (UDRF) the active damping matrix is diagonal. This is a physically uncoupled form of feedback for which each actuator is controlled by the colocated sensor. The instantaneous control force at each actuator location is directly proportional, but opposite in sign, to the instantaneous velocity. This is equivalent to the attachment of a viscous dashpot to the structural DOF of the sensor, with the ratio of controlling force to sensed velocity being the viscous damping coefficient d_{ii} .

For the uncoupled DRF, Horner [12] suggested that the sum of the gains d_{ii} is a measure of control strength to be minimized as the performance measure.

$$f = \sum_{i=1}^{n_c} d_{ii} \tag{3.24}$$

Although this performance index does not have clear physical significance, it was used because it is simple and compatible with uncoupled DRF.

Two quantities are used here as measures of modal control effectiveness or level of damping in the system. One is the damping ratio ζ_r, and the other is the real part of eigenvalue σ_r as defined in Eq. (2.20). Note that the real part of eigenvalue σ is related to the time τ required for the amplitude of vibration to be reduced by the factor of $\frac{1}{e}$ as

$$\tau = -\frac{1}{\sigma} \tag{3.25}$$

The optimum design problem for DRF control cases is formulated as

$$\text{find} \quad \mathbf{D} \tag{3.26}$$

$$\text{to minimize } f(\mathbf{D})$$

$$\text{subject either to } g_j = \zeta_j - \zeta_L \geq 0 \quad j = 1,\ldots, n_m$$

$$\text{or to } g_j = \sigma_U - \sigma_j \geq 0 \quad j = 1,\ldots, n_m$$

$$\text{and } \mathbf{D} > 0 \quad i = 1,\ldots, n_c$$

where ζ_L is minimum required damping ratio, and σ_U an upper limit on the real part. The optimization problem Eq. (3.26) was solved by using a general purpose software package - NEWSUMT-A [54]. NEWSUMT-A is based on a penalty function approach which transforms the constrained optimization problem into a sequence of unconstrained problems. An extended interior penalty function is used together with Newton's method for solving the unconstrained problems.

When the sensors and actuators are coupled the matrix **D** can be full, but we still require symmetry and positive definiteness to insure stability. We call this coupled direct rate feedback (CDRF) control.

A number of performance indices were investigated to obtain the magnitude of the control gains. The minimization of the Euclidian Norm of the gain elements, as suggested in [46], is presented in Appendix C. However, because this performance index does not have a clear physical significance, two new performance indices are proposed in this work.

The first performance index selected here for obtaining the gain matrix **D** is the minimization of the maximum actuator force assuming that each sensor has

the same velocity bound . This control technique will be named Minimum Force Direct Rate Feedback (MF-DRF). The choice of this index is motivated by the fact that the required stability margin limits the response and so the objective function should try minimize the size of the actuators required to achieve the desired stability margins. The force u_i supplied by the i-th actuator is

$$u_i = -\sum_{j=1}^{n_c} d_{ij}\dot{q}_j \tag{3.27}$$

where $\dot{q}_j$ is the velocity measured by the j-th sensor. If $\dot{q}_j$ is bounded by an upper bound $\dot{q}_{max}$, then the maximum possible actuator force u_{max} is proportional to f

$$f = \frac{u_{max}}{\dot{q}_{max}} = \max_i \sum_{j=1}^{n_c} |d_{ij}| \qquad i = 1,...,n_c \tag{3.28}$$

The maximum control force ratio f is minimized subject to constraints on the stability of the closed loop system expressed as lower limits (ζ_L) on the damping ratios ζ_j of the first n_m modes.

Because a maximum function does not have continuous derivatives for MF-DRF, the performance index is approximated as

$$f = [\sum_{i=1}^{n_c} (\sum_{j=1}^{n_c} |d_{ij}|)^p]^{1/p} \tag{3.29}$$

for a large value of p. Furthermore, the absolute value function does not have continuous derivatives at zero and is replaced by a quartic polynomial near zero (i.e. for $|d_{ij}| \leq d_T$), that is

$$f = [\sum_{i=1}^{n_c} (\sum_{j=1}^{n_c} h(d_{ij}))^p]^{1/p} \tag{3.30}$$

where

$$h(d_{ij}) = \frac{d_T}{2} \sum_{i=1}^{n_c} \sum_{j=1}^{n_c} [3(\frac{d_{ij}}{d_T})^2 - (\frac{d_{ij}}{d_T})^4] \qquad \text{for } |d_{ij}| \leq d_T, \tag{3.31}$$

$$h(d_{ij}) = |d_{ij}| \qquad \text{for } |d_{ij}| > d_T.$$

The optimization has to be repeated with increasing values of p in order to converge to an optimum solution. The optimum solution is assumed to be reached for some value of p when the following convergence criterion is satisfied:

$$\left| \frac{f(p_i) - f(p_{i-1})}{f(p_{i-1})} \right| \leq \varepsilon_1 \tag{3.32}$$

Another criterion which is used to define magnitude of p is

$$\|\mathbf{D}_{min} - \mathbf{a}\| \leq \varepsilon_2 \tag{3.33}$$

Following work of Fiacco and McCormick, as described in Ref. 49 on page 138, the position of the minimum of $f(\mathbf{D}, p)$ has the asymptotic form

$$d_{ij\ min}(p) = a_k + \frac{b_k}{p} \qquad as\ p \to \infty \qquad k = 1,...,i + j \tag{3.34}$$

Once optimum has been found for two values of p the vectors **a** and **b** may be estimated and the value of $\mathbf{D}_{min}$ for any other p predicted. To satisfy Eq. (3.34) elements of **a** and **b** are given as

$$a_k = \frac{c\, d_{\text{ij min}}(p_{i-1}) - d_{\text{ij min}}(p_i)}{c - 1} \tag{3.35}$$

$$b_k = [d_{\text{ij min}}(p_{i-1}) - a_k]p_{i-1} \tag{3.36}$$

where $c = \frac{p_{i-1}}{p_i}$.

The aforementioned optimization scheme is rather complex and therefore an equivalent formulation which avoids discontinuity of the objective function was also used. A new variable γ is introduced and the optimization problem is now

$$\text{find} \quad \mathbf{D} \text{ and } \gamma \tag{3.37}$$

to minimize γ

subject to constraints on ζ or σ,

$\mathbf{D} > 0$,

and $\sum_{j=1}^{n_c} |d_{ij}| \leq \gamma \quad i = 1,\ldots,n_c$

A second proposed CDRF control law is called Linear Quadratic Direct Rate Feedback (LQ-DRF) control and is based on the quadratic performance index of the LQ design.

The LQ design minimizes the quadratic performance index for all initial conditions. This is impossible to achieve with direct rate feedback. Instead the

proposed LQ-DRF law minimizes the quadratic performance index for initial conditions in the shape of a number n_m of natural vibration modes. That is

$$J_{LQDRF} = \max_{x_{0i}} \int_0^\infty [q\mathbf{x}(t)^T\mathbf{Q}\mathbf{x}(t) + \mathbf{u}(t)^T\mathbf{R}\mathbf{u}(t)]dt \qquad i = 1,..., n_m \tag{3.38}$$

Additionally, it is required that minimum stability margins be met for those modes by specifying lower limits (ζ_L) on their damping ratios, ζ_i. With LQ design this is commonly achieved by scaling the **Q** or **R** matrices. Because the maximum function in Eq. (3.38) can have discontinuous derivative, an equivalent formulation which also includes scaling of the **Q** matrix is used for the LQ-DRF design as follows:

find q, β and the elements of **D**

to minimize β

$$\text{such that} \quad \int_0^\infty [q\mathbf{x}(t)^T\mathbf{Q}\mathbf{x}(t) + \mathbf{u}(t)^T\mathbf{R}\mathbf{u}(t)]dt \le \beta \tag{3.39}$$

$$\mathbf{x}_0 = \begin{Bmatrix} \mathbf{0} \\ \boldsymbol{\varphi}_i \end{Bmatrix} \qquad i = 1,..., n_m$$

$$\zeta_i \ge \zeta_L \qquad i = 1,..., n_m$$

and $\mathbf{D} > 0$.

Given a set of initial conditions $\mathbf{x}_0$ and q, the quadratic performance index is calculated same way as in Eqs. (3.41)-(3.43) below except that $\bar{\mathbf{Q}}$ matrix is now

$$\bar{\mathbf{Q}} = q\mathbf{Q} + \mathbf{F}_D^T \mathbf{R} \mathbf{F}_D \tag{3.40}$$

and $\mathbf{F}_D$ is the gain matrix for LQ-DRF containing the elements of $\mathbf{D}$ as its only nonzero elements at the DOFs where control pairs are located.

3.2.3 LQ Performance of DRF Designs

For comparison with the LQG design, the quadratic performance index of Eq. (3.1) is calculated for the DRF designs, for a given set of initial conditions $\mathbf{x}_0$ as:

$$J = \mathbf{x}_o^T \bar{\mathbf{P}} \mathbf{x}_o \tag{3.41}$$

where $\bar{\mathbf{P}}$ is obtained from the Lyapunov equation

$$\bar{\mathbf{A}}^T \bar{\mathbf{P}} + \bar{\mathbf{P}} \bar{\mathbf{A}} + \bar{\mathbf{Q}} = \mathbf{0} \tag{3.42}$$

where

$$\bar{\mathbf{A}} = \mathbf{A} - \mathbf{B} \mathbf{F}_D \tag{3.43}$$

and

$$\bar{\mathbf{Q}} = \mathbf{Q} + \mathbf{F}_D^T \mathbf{R} \mathbf{F}_D \tag{3.44}$$

3.3 Design Optimization and Sensitivity

It is assumed that a control system is designed for a structure characterized by a vector **s** of structural parameters such as mass or stiffness of individual elements expressed by their thickness. The control system design is assumed to be a solution of an optimization problem of the form

find **r**

to minimize $f(\mathbf{r}, \mathbf{s})$

subject to some constraints $g_j(\mathbf{r}, \mathbf{s}) \geq 0 \quad j = 1,..., n_g$

where **r** is a vector of control system design variables such as gains **D** and/or control pairs locations, and $g_j(\mathbf{r}, \mathbf{s})$ represents behavioral constraints such as stability limits (i.e. limits on ζ's or σ's) or side constraints such as limits on gains (i.e. **D**). The particular form of the above optimization formulation for different optimality criteria is given in the previous sections. The solution $\mathbf{r}^{opt}(\mathbf{s}_0)$ of the optimization problem for a nominal structure characterized by $\mathbf{s} = \mathbf{s}_0$ is called herein the "DRF Baseline Design". We are interested in the sensitivity of the baseline design to structural modifications, i.e. to changes in the vector **s**.

Two types of sensitivity may be considered. The first is the sensitivity of the baseline design to structural modifications when the control design $\mathbf{r}^{opt}$ is frozen. This type of sensitivity is a measure of the robustness of the design, and is given by partial derivatives

$$\frac{\partial f}{\partial s_k}(\mathbf{r}^{opt}, \mathbf{s}_0), \qquad \frac{\partial g_j}{\partial s_k}(\mathbf{r}^{opt}, \mathbf{s}_0)$$

where s_k is a component of **s**.

The second type of sensitivity derivative measures the change in the optimum design of the control system as the structure is modified. Denoting $f^{opt} = f(\mathbf{r}^{opt}, \mathbf{s})$, we are interested in the derivatives $\frac{\partial \mathbf{r}^{opt}}{\partial s_k}$ and $\frac{\partial f^{opt}}{\partial s_k}$. For the case where the number of active constraints is equal to the number of design variables [49].

$$\frac{\partial \mathbf{r}^{opt}}{\partial s_k} = -(\mathbf{N}^T)^{-1}\frac{\partial \mathbf{g}_a}{\partial s_k} \tag{3.45}$$

where the matrix **N** has components $n_{ij} = \frac{\partial g_{aj}}{\partial r_i}$. The vector $\mathbf{g}_a$ consists of constraints g_{aj} which are active [that is, $g_{aj}(\mathbf{r}^{opt}, \mathbf{s}_0) = 0$] for the baseline design. Similarly, the change in optimized performance is

$$\frac{\partial f^{opt}}{\partial s_k} = \frac{\partial f}{\partial s_k} - \sum_{j=1}^{n_g} \lambda_j \frac{\partial g_j}{\partial s_k} \tag{3.46}$$

where λ_j are Lagrange multipliers obtained at the optimum design of the control system (see below).

To estimate whether a given set of parameter changes $\Delta \mathbf{s}$ will make an inactive constraint g_i become active, a first order Taylor series expansion around the optimum control is used

$$g_i = g_i^{opt} + \sum_{k=1}^{n_p} \frac{\partial g_i}{\partial s_k} \Delta s_k \tag{3.47}$$

The sensitivity of the optimum control design is a measure of the interaction between the design of the structure and the design of the control system. Large values of $\frac{\partial f^{opt}}{\partial s_k}$ indicate that there is a potential for enhancing the control system performance by minor structural modifications.

The Lagrange multipliers λ_j can be found from

$$\mathbf{f}_r - \mathbf{N}\lambda = \mathbf{0} \tag{3.48}$$

where $\mathbf{f}_r$ is a vector of $\frac{\partial f^{opt}}{\partial r_l}$, and λ is a vector of λ_j Lagrange multipliers. If the number (l) of control system design variables (i.e. elements of **D**) is larger than the number of active constraints (j) then the system of linear equations (i.e. Eq. [3.48]) is overdetermined in λ. One may find

$$\lambda = (\mathbf{N}^T\mathbf{N})^{-1}\mathbf{N}^T\mathbf{f}_r \tag{3.49}$$

by minimizing the system residue $\mathbf{r}_E = \mathbf{N}\lambda - \mathbf{f}_r$ (i.e. min of $||\mathbf{r}_E||^2$). The change in performance index due to small change in the structural parameter (Δs_k) can be estimated by the first order Taylor series expansion around its value for optimal baseline design

$$f = f^{opt} + \frac{\partial f^{opt}}{\partial s_k} \Delta s_k \tag{3.50}$$

Chapter 4

Baseline Designs of Control System for a Laboratory Structure

4.1 Analytical Model of Laboratory Structure

The control laws described in the previous sections have been applied to a small laboratory structure. The structure consists of a vertical beam and an attached horizontal crosspiece, with the vertical beam suspended by four cables in tension at its top and bottom (Fig. 1). The crosspiece was designed so that the structure would have third and fourth vibration modes with relatively close natural frequencies. The vertical beam is a uniform steel beam 80 inches long, with a rectangular cross section 2 x 1/8 inch. The crosspiece is an aluminum beam 32 inches long, with a rectangular cross section 2 x 1/8 inch. Small masses consisting

of two ceramic magnets are located at both ends of the crosspiece, which is secured to the vertical beam by a clamp. Each stranded steel suspension cable is 0.09 inch in diameter.

Eight 10-inch beam finite elements with out-of-plane translations and bending rotations as DOFs are used to model the vertical beam. The crosspiece is symmetrical relative to the vertical beam, and only symmetrical out-of-plane motion of the crosspiece is represented in the modeling. The flexible portion of the crosspiece is modeled by two-DOF Rayleigh-Ritz analysis and is shown as spring-mass system in Fig. 2. Therefore, the full-order model has n_n = 19 DOFs. A single string-in-tension finite element represents each cable. The model includes geometric stiffness matrices accounting for tension in the beam elements. The tension in the beam is proportionally reduced down the beam by the effect of gravity. Small lumped masses representing the control system coils, cable clamps, and the crosspiece clamp are added to the model. Inherent damping equivalent to the measured open loop damping of the structure was included in the analysis of the structure. The lowest six open loop damping ratios are: 0.0045, 0.0020, 0.0039, 0.0019, 0.0029, 0.0012, and the remaining damping ratios are modeled to be zero. Complete details of the modeling are given in Ref. 55. Because of control hardware limitations for LQG a reduced model of the system was also required. Only the ten translation DOFs and the lowest ten modes (i.e. n_R = 10) were retained.

The six lowest modes of the laboratory structure are of primary interest. Their calculated and measured natural frequencies and calculated mode shapes are shown in Fig. 2.

Control of the structure is effected by feedback involving three force actuators, each colocated with a velocity sensor (i.e. $n_c = n_s = 3$) as indicated by coil pairs shown on Figs. 1 and 2. The instantaneous control force at each actuator location is dependent on the control scheme being implemented.

4.2 Experimental Apparatus and Procedure

Experiments were conducted to test the accuracy of the theoretical predictions against laboratory measurements of the control system performance. All the control schemes (DRF and LQG) described in the previous sections were tested on the structure using identical control hardware. Displacement frequency response functions (DFRFs) were measured at three positions along the beam and compared with theoretical DFRFs for the same locations.

The basic experimental apparatus and procedures are described in detail in Ref. 55. A summary of the apparatus used and the procedure relevant to this study is provided here.

Each noncontacting velocity sensor and force actuator consists of a small structure-borne coil which moves within an annular magnetic field generated by an externally supported magnetic field assembly. Movement of a velocity sensing

coil through the magnetic field produces a voltage proportional to the velocity, and application of a current to a force actuator coil produces a proportional control force. A Systolic Systems Inc. PC-1000 digital analyzer is used as a controller, and is operated through a host IBM-PC personal computer. The personal computer is also used to load discretized form of control design to the controller. The PC-1000's array processor performs one specific operation -- multiplication of a constant 48 x 48 coefficient matrix by a time-varying 48 x 1 vector -- at the specified sampling rate. The constant matrix contains discretized information about the control system design and the time varying vector consists of discretized sensed output and internal state variables. The product of two is a vector containing control command and updated reconstructed state. An STI-11/23 data acquisition and analysis system developed by Synergistic Technology Inc. generated excitation signals, received measurement sensor signals, and performed all data analysis.

DFRFs were measured at grid points 4, 6, and 8 on the vertical beam. The displacement sensors used were noncontacting inductive-type proximity probes. Random excitation was used. Fast Fourier transforms of the response and excitation signals were calculated, and the former was divided by the latter to produce a DFRF.

4.3 Analytical Results for UDRF Control

The control system was designed for the cruciform beam so as to minimize the sum of the d_{ti} supplied by the three actuators (see Eq. [3.24]). The design variables were the values of individual d_{ti} and the locations of the sensor-actuator pairs. The requirements imposed on the control system were $\zeta_j \geq 0.03$ for the first six modes, j = 1,...,6. The control optimization procedure produced the baseline design [$\mathbf{r}^{opt}(\mathbf{s}_0)$] shown in Table 1 with the sensor-actuator locations almost exactly at grid points 5, 7 and 9. The fourth, fifth and sixth damping ratios (ζ_4, ζ_5, ζ_6) were at the lower limit of 0.03 while the first three damping ratios were above this value.

Instead of imposing constraints on damping ratios, i.e. on the number of cycles required for decay of vibration, one can possibly impose constraints on time τ_r of vibration decay by constraining the real parts of eigenvalues σ_r. Required upper limit on real part of eigenvalues for first six lowest frequency modes was $\sigma_r = 0.03\omega_6 = -4.28\ s^{-1}$. This is equivalent to the decay time of $\tau_r = 0.23$ s. Two designs are shown in Table 2: one with three control pairs at grid points 5, 7 and 9, and the other with two control pairs at grid points 5 and 9. In the first design, the optimizer has eliminated completely control pair at grid point 7 and therefore design with two control pairs was performed there after. Grid points 7 and 9 are also optimal location for control pairs. In both designs the upper limit on σ_4 was the active constraint, which means that the fourth mode is controlling the design.

4.4 Analytical Results for CDRF and LQG Control

Two CDRF control systems, i.e. the MF-DRF system and the LQ-DRF system, were designed with the requirement that the lowest six closed loop modes have damping ratios of at least 0.03 (i.e. $n_m = 6$ and $\zeta_L = 0.03$). This stability margin requirement was applied in the case of LQ-DRF design through selection of $q\mathbf{Q}$ and $\mathbf{R}$ matrices. Two optimization problems (see Eqs. [3.37] and [3.39]) for the respective control systems were solved by using NEWSUMT-A. The control optimization procedure produced the designs **D** shown in Table 3 for the MF-DRF control, and in table Table 4 for the LQ-DRF control. Damping ratios of the six lowest closed loop modes are shown in columns MF-DRF and LQ-DRF of Table 5. For the fixed values of $\mathbf{Q} = \mathbf{I}$ and $\mathbf{R} = 0.22\mathbf{I}$, the optimum value of q was 0.0001 and the maximum value of J was realized for the sixth mode (LQ-DRF control). The small value of q indicates that the LQ-DRF system was designed to minimize control effort (the $\mathbf{u}^T\mathbf{R}\,\mathbf{u}$ term in the quadratic performance index) with system response bounded by the required stability margin.

Next, the LQR control system was designed with **Q** selected to be the identity matrix, and **R** a scalar matrix ($\mathbf{R} = 0.22\mathbf{I}$) selected to be just large enough to achieve at least 3% damping in the lowest six modes of vibration. The filter design was obtained for $\mathbf{V}_1 = 10^{-6}\mathbf{I}$, $\mathbf{V}_2 = 5x10^{-4}\mathbf{I}$, and $\alpha = 0.2\ cs^{-1}$ Table 5 shows the damping ratios for both the full-order LQR design and for the reduced model regulator/filter design (obtained from the eigenvalues of $\mathbf{A}_E$, Eq. [3.19]).

It is seen that for the lowest six modes with the imposed stability margin, the model reduction and the Kalman filter have very little effect on the damping ratios. The LQR damping ratios are greater than the corresponding values for the CDRF designs, indicating that more control effort is supplied by the LQ regulator than by the CDRF controllers.

The effect of model reduction on the dynamics of the unmodeled modes is explored next. Table 6 compares the roots of the regulator for the full-model and reduced-model designs. Also given in Table 6 are the roots of the filter for the full-order design and the roots of the CDRF designs. Comparing the roots of the full-order and the reduced-order designs, we note that the differences in the modeled modes (first ten) are very small. However, the unmodeled modes lose almost all of their stability margins, and we were fortunate that these modes did not become unstable (the spillover instability). The CDRF designs, by comparison, provided all the modes with significant stability margins, some comparable to those of the controlled modes. This is a major advantage of the CDRF design over the LQG design, an advantage likely to be more dramatic for real-life systems for which the ratio of modeled to unmodeled modes is much smaller.

It is also seen from Table 6 that all the filter roots had real parts of approximately -40 s^{-1} indicating good separation of filter poles from the regulator ones and fast state variables restoration. This held for the reduced-order design except that the reduced-order filter had only ten roots. The value of -40 s^{-1} is equal to 2α ($\alpha = 0.2\,cs - 1$) . instead to α because α is large compared to V_1 (see Appendix B).

The quadratic performance index (see Eqs. [3.4], [3.14], and [3.41]) was calculated using the $q\mathbf{Q} = \mathbf{I}$ and $\mathbf{R} = 0.22\,\mathbf{I}$ obtained for the LQ design and for initial conditions in the shape of the first six open loop mode shapes, and the results are presented in Table 7. Results are presented only for the full model because the effect of model reduction for the controlled modes is minimal. The comparison of the LQR and LQG columns shows that the deterioration in performance due to the need for an observer is significant only for the higher modes. Comparison of the LQG and MF-DRF columns shows that the optimal control law is better for the first four modes and poorer for the fifth and sixth mode. The maximum value of the index is almost the same for the two control laws. Comparison of the LQG and LQ-DRF columns shows that even though the comparison is made for the LQ index ($q\mathbf{Q} = \mathbf{I}, \mathbf{R} = 0.22\,\mathbf{I}$) the LQ-DRF design is comparable or better, with the maximum value of the index being substantially lower. Basically, the loss of performance due to state reconstruction for the LQG outweighs the loss due to a suboptimal (and simpler) LQ-DRF design.

The displacements and velocities (controlled by the LQG and MF-DRF control) at the midpoint of the vertical beam for the first and fifth mode initial conditions are shown in Figs. 3-6, and the actuator forces are compared in Figs. 7-10. In general it is observed that the optimal control law results in smaller displacements but also larger forces. This is expected as the optimum control law minimizes an index which depends on both displacements and forces while the MF-DRF law minimizes only the control-force ratio.

Finally, the optimization problem of minimizing maximum actuator force (see Eqs. [3.26] and [3.30]) was performed with constraints placed on the first six real parts of the lowest eigenvalues (with $\tau = 0.23s$), and the optimizer produced the baseline design matrix **D** (with p = 9 in Eq. [3.30]) shown in Table 8. The performance index for this design is equal to 0.1655 lb-s/in. The real parts of the second, fourth and fifth pair of eigenvalue values reached upper limit.

4.5 Comparison of Analytical and Experimental Results

CDRF vs. LQG Control

Representative DFRF magnitudes, for the open-loop system and the closed-loop system using the MF-DRF, LQ-DRF and LQG control laws, are plotted on Fig. 11 (A, C, E and G) for experimental measurements at grid point 6 and excitation at grid point 9. The corresponding theoretical DFRF magnitudes obtained for the full-order model are plotted on Fig. 11 (B, D, F and H). The open loop theoretical results and measurements (Fig. 11 B and A) verify the natural frequencies of the theoretical model (i.e. 1.9 Hz, 4.8 Hz, and so on), and show realistic modeling of structural damping (which was based on experimental measurements). Good agreement of theoretical and experimental MF-DRF control response is observed by comparing Fig. 11 D and C. For example, at 1.76 Hz (first peak) the theoretical DFRF magnitude is 0.88 (in/lb) and the experiment shows magnitude of 0.86 (in/lb), for 4.8 Hz (second peak) the respective

DFRF magnitudes are 0.11 and 0.13 (in/lb), for 8.6 Hz (third peak) the DFRF magnitudes are both 0.16 (in/lb), and for 19.5 Hz (antiresonance) they are 0.022 and 0.020 (in/lb) respectively. The theoretical and experimental LQ-DRF control response also compare well (Fig. 11 E and F). At 1.51 Hz the theoretical DFRF magnitude is 0.88 (in/lb) and so is the experimental one, for 5.21 Hz the respective DFRF magnitudes are 0.077 and 0.085 (in/lb), for 8.4 Hz DFRF magnitudes are 0.099 and 0.098 (in/lb) respectively, and for 18.9 Hz are same 0.021 (in/lb). The agreement for the LQG design (Fig. 11 F and E) is as good. For example, for 5.6 Hz (second peak) the DFRF magnitudes are 0.82 and 0.9 (in/lb), and for 22.7 Hz (last peak) they are 0.044 and 0.054 (in/lb).

Comparison of the open loop system plots with closed loop plots shows that the closed loop DFRF magnitude peaks are at least one order of magnitude smaller than respective open loop peaks indicating heavy control damping in the system. A magnitude of control damping per controlled mode may be inferred from a resonant peak roundness and matches with values of respective damping ratios shown in Table 5.

Table 1. Controller gains (lb-s/in) and performance index for UDRF designs with constraints on damping ratios

Gain *	Uniform Gain Design	Baseline Design	Added (node 8) Mass Design	Variable Thickness Design
d_{11}	0.01188	0.06289	0.06248	0.05378
d_{22}	0.01188	0.01165	0.00000	0.00000
d_{33}	0.01188	0.02870	0.03272	0.03134
Σd_{ii}	0.03564	0.10324	0.09520	0.08512

* With sensor-actuator pairs located at grid points 5, 7 and 9

Table 2. Controller gains (lb-s/in) and performance index for two UDRF designs with constraints on decay time

Gain	Three Control* Pairs Design	Two Control** Pairs Design
d_{11}	0.2322	0.2324
d_{22}	0.0001	
d_{33}	0.1195	0.1195
Σd_{ii}	0.3517	0.3519

* With sensor-actuator pairs located at grid points 5, 7 and 9

** With sensor-actuator pairs located at grid points 5 and 9

Table 3. Gain matrix D for MF-DRF control (lb-s/in)

Actuator Grid Pt. No.	Sensor Grid Pt. No.		
	5	7	9
5	0.0500	0.0000	0.0000
7	0.0000	0.0359	-0.0139
9	0.0000	-0.0139	0.0222

Table 4. Gain matrix D for LQ-DRF control (lb-s/in)

Actuator Grid Pt. No.	Sensor Grid Pt. No.		
	5	7	9
5	0.0581	0.0261	-0.0011
7	0.0261	0.1018	-0.0014
9	-0.0011	-0.0014	0.0448

Table 5. Closed Loop Damping Ratios

Mode No.	LQR	LQG Reduced-model Design	MF-DRF	LQ-DRF
1	0.6221	0.6216	0.1830	0.5589
2	0.2270	0.2270	0.0304	0.0695
3	0.1441	0.1437	0.0600	0.1151
4	0.0666	0.0666	0.0301	0.0428
5	0.0567	0.0563	0.0454	0.0613
6	0.0301	0.0298	0.0300	0.0300

Table 6. Closed Loop Roots (1/s)

Mode No.	LQG Full-Model Design				LQG Reduced-Model Design		MF-DRF		LQ-DRF	
	Regulator		Filter		Regulator					
	Real Part	Imaginary Part	Real Part	Imaginary Part	Real Part	Imaginary Part	Real Part	Imaginary Part	Real Part	Imaginary Part
1	-14.30	18.	-40.05	11.	-14.30	18.	-2.14	11.	-6.61	10.
2	-7.24	31.	-39.98	30.	-7.24	31.	-0.92	30.	-2.10	30.
3	-8.11	56.	-39.89	55.	-8.09	56.	-3.35	56.	-6.44	56.
4	-3.97	59.	-39.92	59.	-3.97	59.	-1.77	59.	-2.50	58.
5	-5.14	90.	-39.88	91.	-5.10	90.	-4.11	90.	-5.53	90.
6	-4.30	143.	-40.03	143.	-4.26	143.	-4.28	142.	-4.27	142.
7	-2.37	232.	-40.15	232.	-2.33	232.	-0.78	232.	-1.42	232.
8	-3.76	316.	-40.66	316.	-3.67	316.	-2.69	316.	-3.83	316.
9	-2.61	432.	-40.49	432.	-2.52	432.	-0.83	432.	-2.94	432.
10	-3.58	575.	-41.23	575.	-3.48	575.	-2.83	575.	-4.55	575.
11	-1.03	821.	-41.55	821.	-0.1358	821.	-0.39	821.	-0.73	820.
12	-2.40	994.	-44.13	994.	-0.1625	994.	-2.05	993.	-3.00	993.
13	-1.68	1287.	-41.91	1287.	-0.1905	1287.	-0.68	1287.	-0.94	1287.
14	-2.78	1560.	-45.65	1560.	-0.0122	1560.	-1.83	1560.	-1.92	1560.
15	-1.71	1919.	-42.65	1919.	-0.0251	1919.	-0.44	1919.	-0.67	1919.
16	-2.60	2403.	-45.42	2403.	-0.0292	2403.	-1.25	2403.	-1.39	2403.
17	-1.66	3040.	-41.89	3040.	-0.0022	3041.	-0.13	3040.	-0.47	3040.
18	-2.95	3366.	-45.24	3366.	-0.0023	3367.	-0.50	3367.	-1.13	3367.
19	-0.75	3622.	-40.35	3622.	-0.0005	3622.	-0.05	3622.	-0.08	3622.

Table 7. Quadratic Performance Index

Initial Conditions Mode No.	LQR	LQG	MF-DRF	LQ-DRF
1	43.	56.	97.	63.
2	39.	44.	144.	72.
3	27.	34.	45.	32.
4	38.	48.	57.	46.
5	62.	78.	65.	69.
6	108.	145.	113.	110.

Table 8. Gain matrix D for MF-DRF control (lb-s/in) constraints imposed on decay time

Actuator Grid Pt. No.	Sensor Grid Pt. No.		
	5	7	9
5	0.1460	0.0001	0.0146
7	0.0001	0.0943	0.0443
9	0.0146	0.0443	0.0561

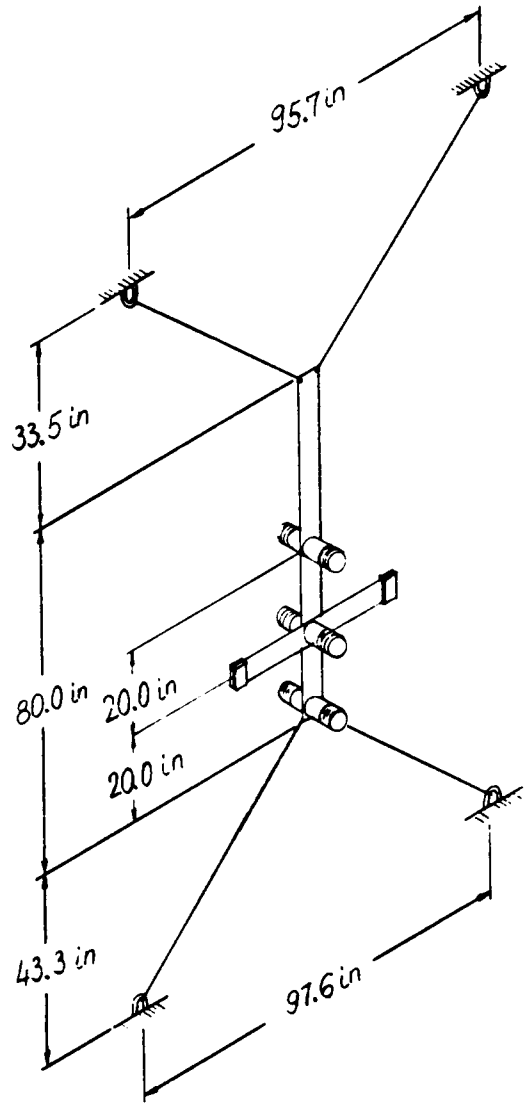

Figure 1. Geometry of the laboratory structure

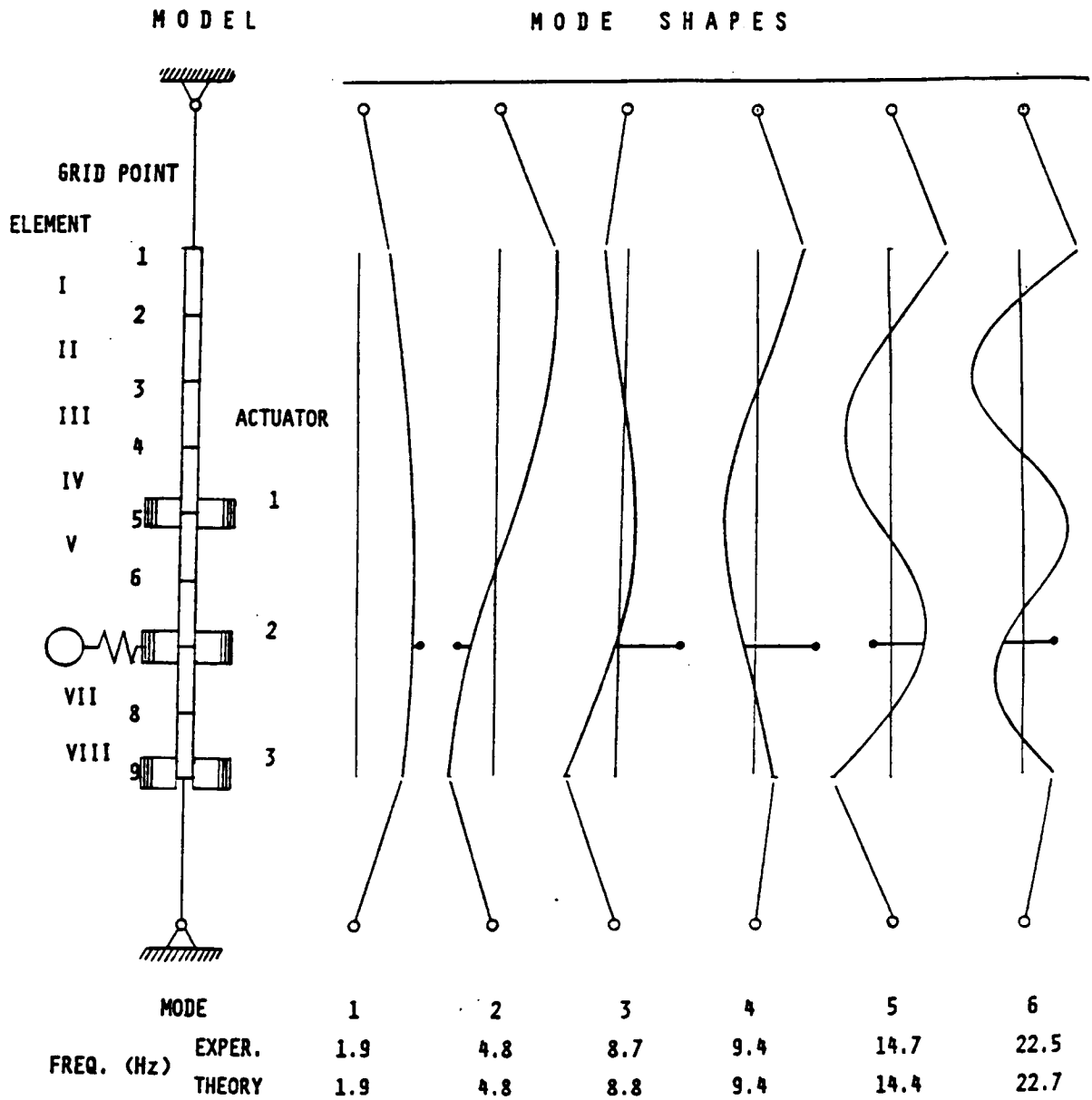

Figure 2. Finite element model and mode shapes

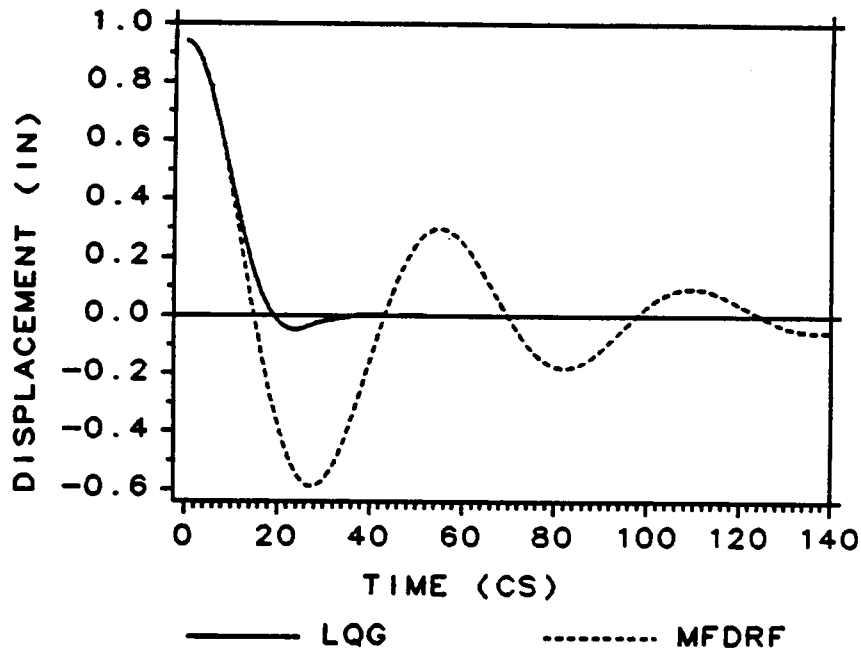

Figure 3. Displacement of mid-point of vertical beam with first-mode-shape initial conditions

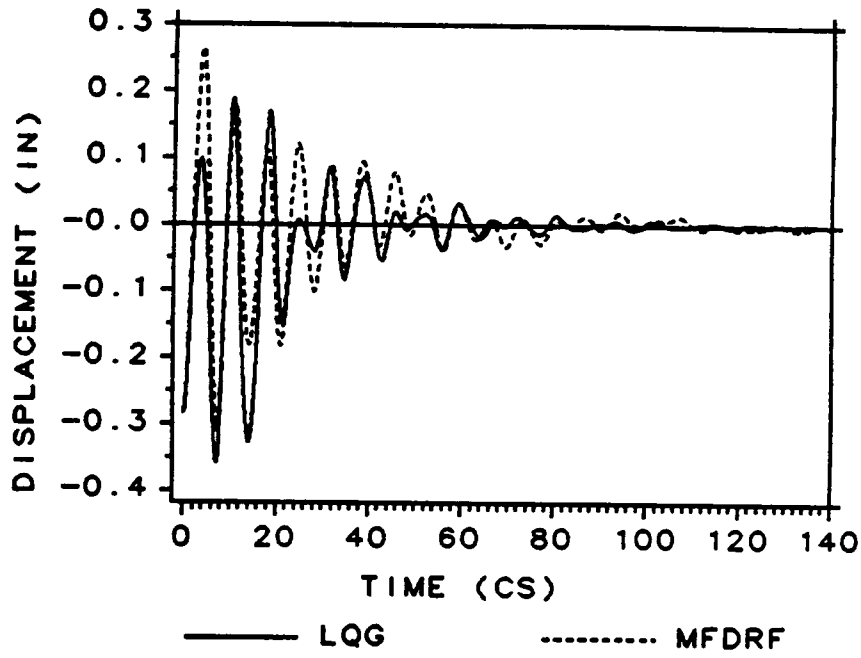

Figure 4. Displacement of mid-point of vertical beam with fifth-mode-shape initial conditions

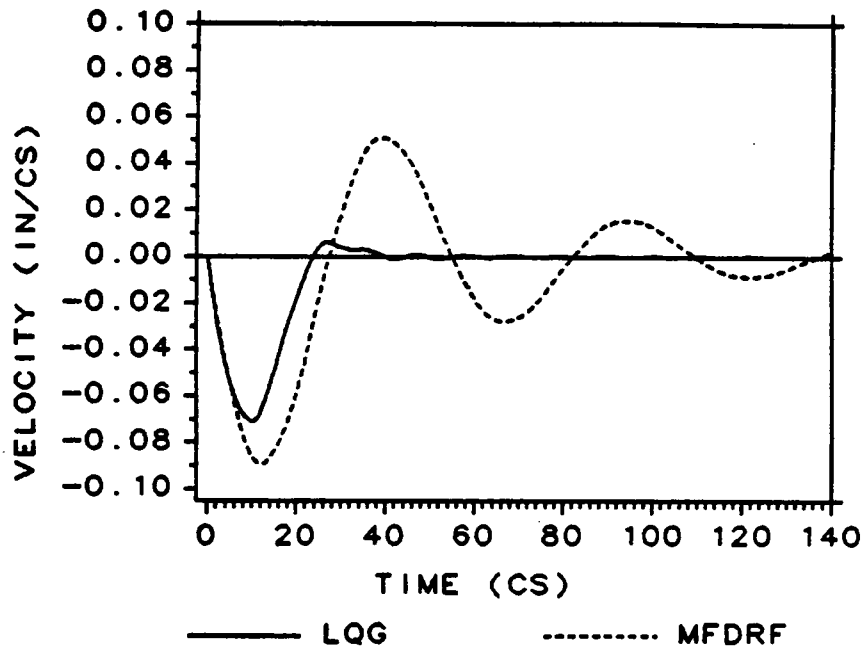

Figure 5. Velocity of mid-point of vertical beam with first-mode-shape initial conditions

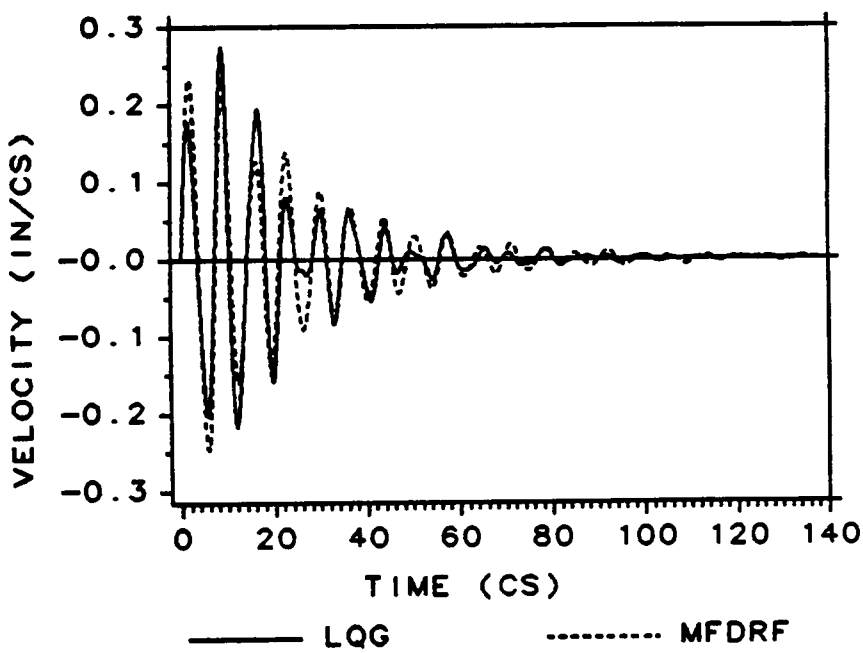

Figure 6. Velocity of mid-point of vertical beam with fifth-mode-shape initial conditions

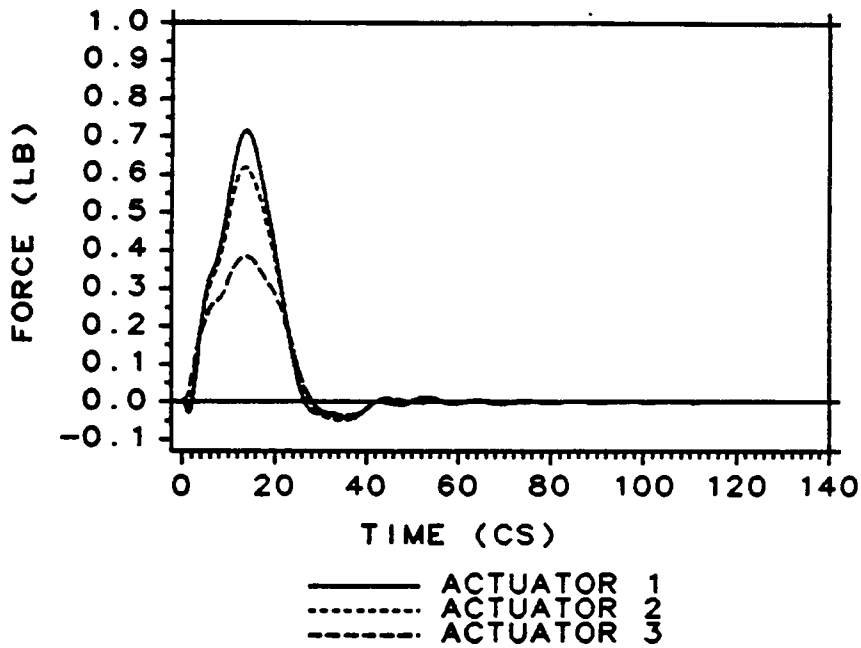

Figure 7. Control forces for LQG controller with first-mode-shape initial conditions

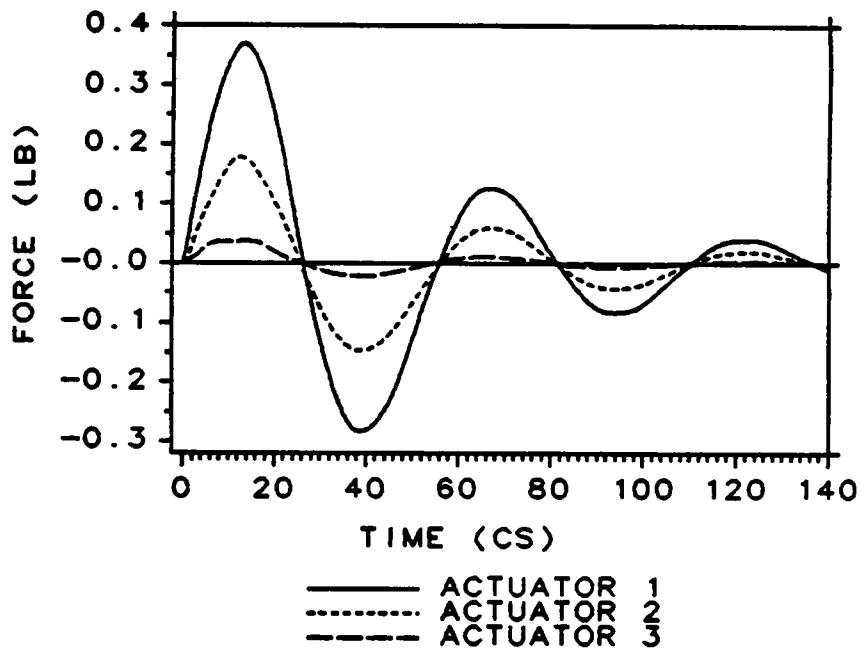

Figure 8. Control forces for MF-DRF controller with first-mode-shape initial conditions

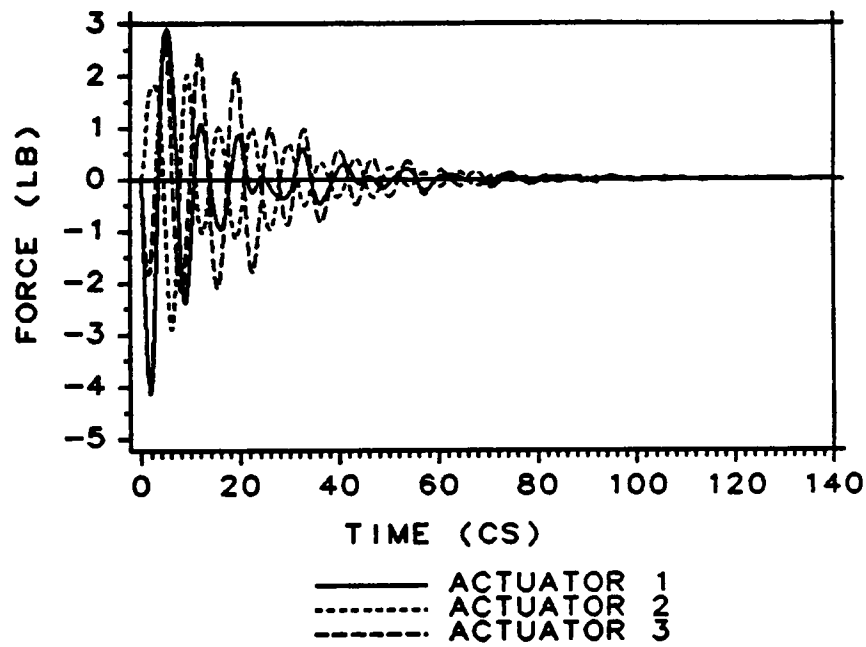

Figure 9. Control forces for LQG controller with fifth-mode-shape initial conditions

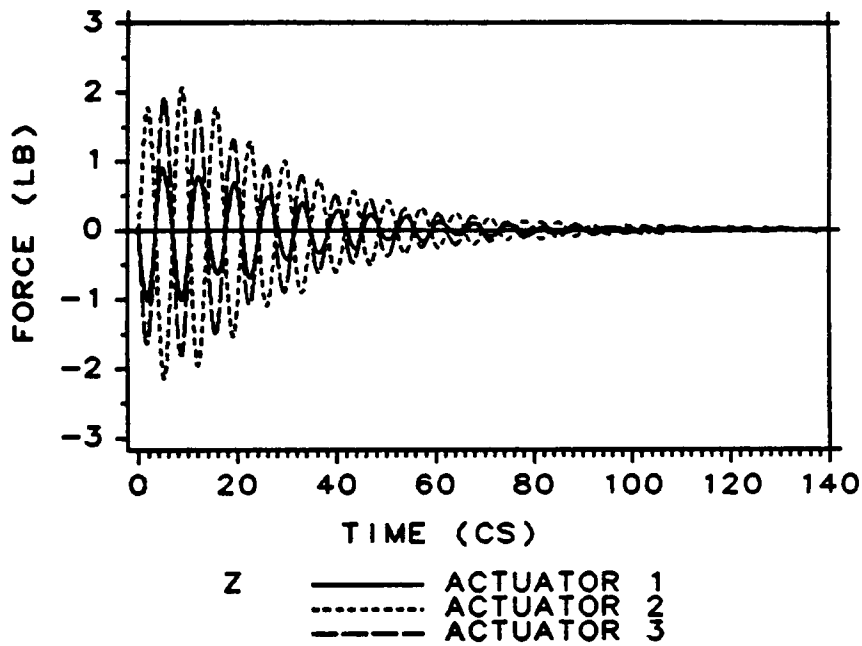

Figure 10. Control forces for MF-DRF controller with fifth-mode-shape initial conditions

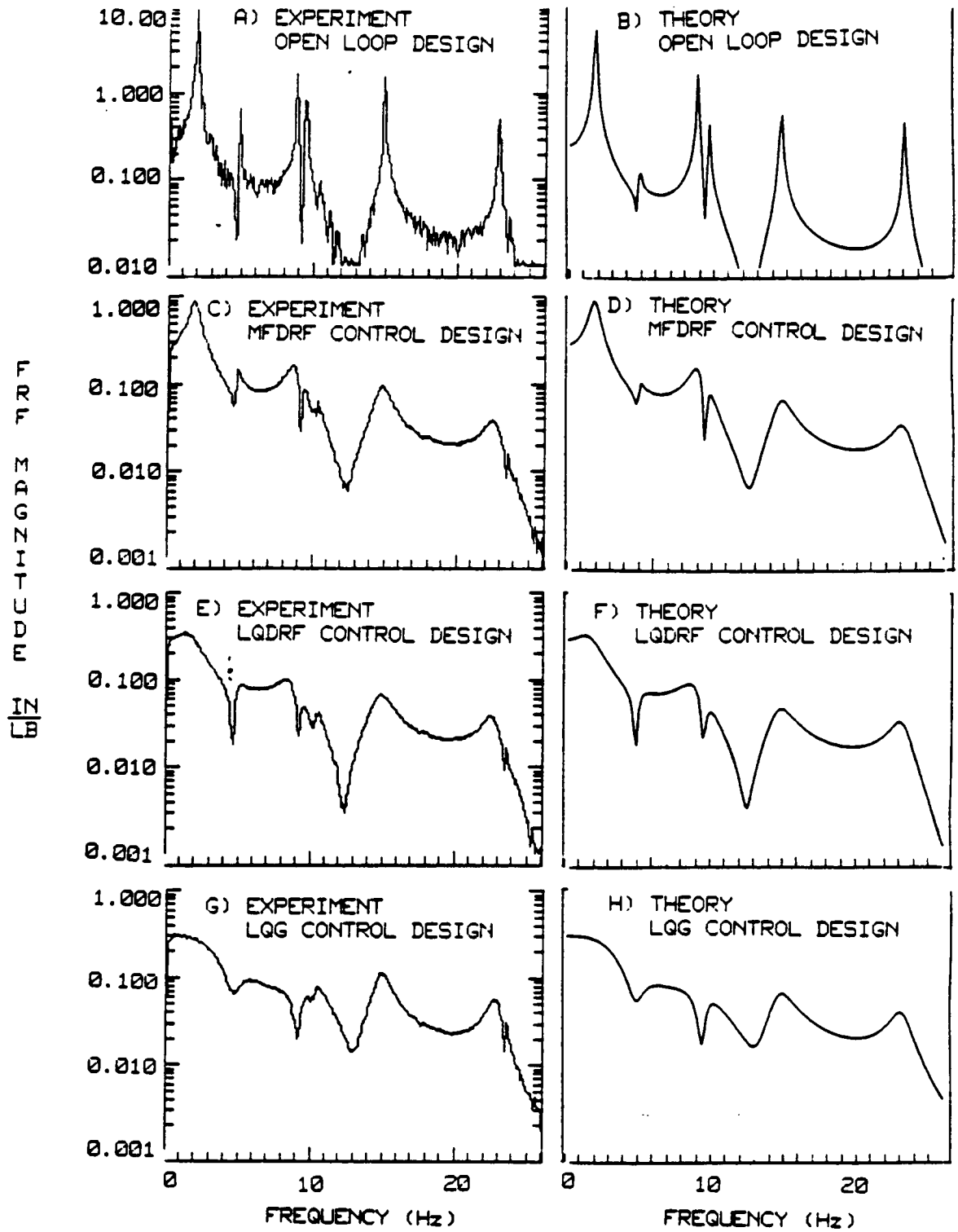

Figure 11. Experimental and theoretical translation-to-force FRF of response at grid point 6 due to excitation at grid point 9: open loop system (A and B), MF-DRF design (C and D), LQ-DRF design (E and F), and LQG design (G and H).

Chapter 5

Effects of Small Structural Changes and Model Reduction on Control System Design and Performance

5.1 Sensitivity Considerations

Two aspects of the sensitivity of the control system to minor structural modifications are investigated. The first is the sensitivity of the performance/stability of the control system, which is associated with the robustness of the system. The second is the sensitivity of the optimum design of the control system, which is important in the assessment of the need for combined control/structural design. Here, it is assumed that the control system is first optimized for maximum per-

formance for the original structural configuration, and then sensitivity analysis of optimized system is used to predict the changes in the performance or stability due to structural modification.

In addition to performance/stability sensitivity to changes in structure, sensitivity of control system to structural model reduction (or stability robustness) is investigated. One of the fundamental problems in the Large Space Structures control is how to control an infinite-dimensional structure with a low-order controller. Structural model reduction in control system design is imposed by physical and hardware limitations of the controller. Consequently, the control system is designed based on a reduced order model of the structure including a first few vibration modes. The modal truncation of the structural model can result in a control system which destabilizes higher order modes, a phenomenon known as spillover instability [5].

5.2 Sensitivity of UDRF Control

The structural design parameter vector **s** was chosen to represent small additional masses m_k at the nine grid points of the finite element model. This choice was motivated by the ease of implementing the change experimentally. The robustness type sensitivity $\frac{\partial g_j}{\partial m_k}(\mathbf{r}^{opt}, \mathbf{s}_0)$ was calculated by computing the derivatives of the three critical damping ratios $(\frac{\partial \zeta_4}{\partial m_k}, \frac{\partial \zeta_5}{\partial m_k}, \frac{\partial \zeta_6}{\partial m_k})$ with respect to the additional mass. The results are presented in Table 9, normalized to show the

expected change in damping ratios $\Delta\zeta_j$ effected by adding a concentrated mass m_k which is 1% of the total mass of the structure. The results in Table 9 indicate that adding the small mass at grid point 1 can reduce ζ_4 from 0.03 to 0.02 so that the control system is not at all robust.

Next, the optimum sensitivity calculations ($\frac{\partial f^{opt}}{\partial m_k}$) were performed. Here Eq. (3.46) becomes

$$\frac{\partial f^{opt}}{\partial m_k} = -\sum_{j=1}^{6} \lambda_j \frac{\partial g_j}{\partial m_k} = -\sum_{j=1}^{6} \lambda_j \frac{\partial \zeta_j}{\partial m_k} \tag{5.1}$$

The sensitivity of the objective function to the additional 1% mass $[\Delta(\Sigma d_{ii})^{opt} = \frac{\partial f^{opt}}{\partial m_k} m_k]$ is given in Table 10. It shows that an additional mass at grid point 1 has the most detrimental effect, increasing the objective function by 23%, while an added mass at grid point 8 has the most beneficial effect, reducing the objective function by 3.9%.

The results of the sensitivity prediction were checked by redesign of the control system for a modified structure. A mass corresponding to 0.86% of the total mass of the structure was added at grid point 1. Table 11 compares the sensitivity analysis predictions to results obtained by reoptimizing the control system for the modified structure. The agreement between the sensitivity predictions and the reoptimized results is very good.

In enhancing the control system performance the sensitivity calculation $\frac{\partial \mathbf{r}^{opt}}{\partial m_k}$ showed that the gain of the second actuator is reduced as the mass is added to grid point 8. The mass that was added to this grid point was chosen to make this gain equal to zero and corresponds to 2.0% of the total mass of the structure.

It is predicted to improve the objective function by 7.7% (see Table 1). Increasing the mass further is not helpful because the gain of the second actuator cannot be reduced below zero. However, the improvement of 7.7% is considered to be substantial for such a minor change in the mass.

Re-optimization was performed with constraints on the sum of nine masses to be equal to or less than 2.0% of mass of the structure, and the results showed good agreement with the sensitivity prediction given in Table 1. Increasing the limits of the permitted mass change was also tried, but brought only small additional improvements in performance.

The beam thickness of t_k of the eight finite elements were chosen next to be structural design parameters s. The Lagrange multipliers were calculated for the three active constraints, and $\frac{\partial f^{opt}}{\partial t_k}$ was evaluated using equation analogous to Eq. (5.1).

$$\frac{\partial f^{opt}}{\partial t_k} = - \sum_{j=1}^{6} \lambda_j \frac{\partial \zeta_j}{\partial t_k} \tag{5.2}$$

The sensitivity derivatives of the performance index with respect to the thickness of each element are shown in Table 12. Changes in control gains d_{ii} (i = 1,2,3) due to changes in design parameters t_k were also calculated from Eq. (3.45) in order to estimate limits to the sensitivity analysis predictions. It was found that the most critical constraint limiting the range of application of the sensitivity analysis was the requirement that d_{22} remain positive, see Table 13 for the sensitivity of d_{22} to changes in thickness.

It can be seen from Table 12 that the thickness of the topmost element has the largest sensitivity derivative of the performance index, and therefore changes in this thickness produce the greatest improvement of the performance index for a given structural change. However by using the linear approximation [Eq. (3.47)], the constraint that d_{22} must remain positive limits the maximum reduction in t_1 to $\dfrac{d_{22}^{opt}}{\dfrac{\partial d_{22}}{\partial t_1}} = 7.44x10^{-3}$ inch or 5.9% relative to its baseline design. This decrease in thickness of the first element would bring reduction in total gain by only 6.2% and indicates that thickness of other elements have to be changed in order to achieve further reductions in the performance index.

The structure-control system was reoptimized with control gains and thickness used as the design variables and with changes in thickness limited to 10% of the baseline values. The optimization results are shown in Table 14 and the controller gains are listed in Table 1. The performance index was reduced to 0.08512 lb-s/in or 17.5% compared to the baseline design control gain, while the sensitivity analysis based on the thickness changes given in Table 14 and the derivatives in Table 12 predicts a value of 0.08760 lb-s/in, which is quite close. The total reduction of the mass of the structure is less than 3.7%. Lower limits (0.03) were reached on the fourth, fifth, and sixth damping ratios and $d_{22} \geq 0.0$ also becomes an active constraint.

These results indicate that the potential for harmful interaction is very large, but there is also a significant potential for beneficial interaction. Thus, the results

indicate that for this case simultaneous structures/control design may be indicated.

Sensitivity of the UDRF Control to small structural changes with eigenvalue real parts (time decay) constrained was investigated for two control pairs design. Table 15 shows mass sensitivity $\frac{\partial f^{opt}}{\partial m_k}$. The grid point 9 has the most negative derivative and sensitivity analysis predicts 1.8% change in performance index for 1% added mass at that location. The reoptimization process shows drop of 2.2% in the performance index. Table 16 shows thickness sensitivity $\frac{\partial f^{opt}}{\partial t_k}$. Using the first order Taylor series expansion around the optimal point, one finds that 6% reduction in thickness of finite element 7 would cause reduction of 3.8% in the performance index. The reoptimization program for the same conditions produced reduction of 3.2% of performance index. If all eight elements were allowed to change no more than ± 5% the optimization would produce the design shown in Table 17 and reduction of 9.7% in performance index. This design has reduction of 2.3% in the total mass of the structure.

5.3 Experimental Results and Comparison with Theory for UDRF Control

An experimental study was done to check effect of small structural changes on the UDRF control design. Three control gains are shown in Table 1: uniform gain design, baseline design, and added mass at node 1 or 8 design. First, an

unoptimized control design consisting of the uniform gains was tested to validate the theoretical model before any optimization was performed. Second, the baseline case was tested, and third, the baseline with added mass designs was tested.

The prediction that a small mass at grid point 1 has a large detrimental effect on the performance of the system was checked by adding 1.31% of the total mass of the structure at that location. The choice of the magnitude of the mass was based on convenience in the experimental verification. Table 18 compares the analytical predictions and experimental measurements of the effects of the added mass. There are substantial differences between predictions and measurements for the third and fifth modes, but in general the agreement is good. In particular it is clear that the additional mass severely reduces the damping ratio for the fourth mode as predicted by the analysis. These results validate the theoretical prediction of the large detrimental effect of a small mass on the performance of the UDRF control system.

Table 19 compares the analytical predictions and experimental measurements for the other three designs. The agreement is very good for the uniform-gain design and is fairly good for the other two designs. The poorer agreement of the optimized designs may be expected because the optimization process tends to capitalize on second order effects that are more poorly modeled. However, the agreement is close enough to validate the analytical predictions.

5.4 Effect of Small Structural Changes on CDRF (MF-DRF) Control Design

An investigation of influence of small structural changes on the performance of the MF-DRF control system was done similar to one done for UDRF control. This part of the study was performed with slightly suboptimal MF-DRF baseline design obtained using p = 11 in formulation of Eq. (3.30). **D** shown in Table 20 is not much different from the truly optimal one shown in the Table 3. Active constraints were $\zeta_2 = \zeta_4 = \zeta_6 = 0.03$.

The effect on the control system performance of small mass added at one of nine possible grid points was investigated first using the sensitivity analysis. In our case, number of control system design variables is $l = 1,...,6$ (i.e. elements of **D**) and the number of active constraints is j = 1,2,3. This leads to the overdetermined system of linear equations (i.e. Eq. [3.48]) in λ. The change in performance index due to small change in the structural parameter (Δm_k) can be estimated by Eq. (3.50). Sensitivities $\frac{\partial f^{opt}}{\partial m_k}$ for nine possible locations of a lumped mass are given in Table 21. 1% added mass of whole structure (0.00022236 lb-s^2/in) at grid point 3 would cause reduction of the performance index from 0.0519 to 0.0502 (lb-s/in) or by 3.4%. The sensitivity prediction result was checked by adding the same lumped mass at grid point 3 and letting optimizer find minimum value of the performance index for the same set of constraints as before. The performance index was reduced by 2.9% which is fairly close to 3.4% predicted

reduction by the sensitivity analysis. This change in performance is not dramatic, but depending on whether one could accept 3.4% improvement in the system performance due to increase in 1% of the mass as significant, it may indicate a synergetic effect if structure and control were designed simultaneously.

Robustness type sensitivity analysis ($\frac{\partial \zeta_4}{\partial m_k}$) shows that 1% added mass at the top of the beam would reduce ζ_4 from 0.03 to 0.022 (see Table 22) which indicates that MF-DRF control design is more robust than UDRF control design where ζ_4 was reduced to 0.020.

The sensitivity of the design with constraints on the decay time τ_r was investigated next. Required upper limit on real part of eigenvalues for first six lowest frequency modes was -4.28 s^{-1}. This is equivalent to the decay time of 0.23 s. The design with added masses was investigated. The sensitivity analysis predicted that the most beneficial effect on control system performance would have small mass added at grid point 9. However, this effect is very small, 1% added mass would result in 1.05% reduction in the performance index. Similar reduction of 1.09% was obtained in optimization process used for checking the sensitivity prediction with 1% of total structural mass added to the bottom of the beam (i.e. grid point 9).

The above results indicate that small change in the structural design variables had no practical effect on control and that the synergistic effect is not significant.

5.5 *Performance Robustness of the LQG Control*

The sensitivity of the baseline design performance to small changes in the structure was investigated considering two alternatives.

The first alternative, called the Updated Model (UM) approach considers how the control system will perform if the controller is designed for the baseline model but the observer works with knowledge of changes in the structure (i.e. structural changes are accounted for in the filter equation). See control system block diagram on Fig. 12 a.

We represent minor changes in the structure by adding a small lumped mass to the vertical beam and we evaluate consequent changes in the quadratic performance index. This effects change in the system and control matrices

$$\mathbf{A}_m = \mathbf{A} + \Delta\mathbf{A} \qquad \mathbf{B}_m = \mathbf{B} + \Delta\mathbf{B} \tag{5.6}$$

or

$$\mathbf{A}_m = \begin{bmatrix} -(\mathbf{M}_s + \Delta\mathbf{M}_s)^{-1}\mathbf{C}_s & -(\mathbf{M}_s + \Delta\mathbf{M}_s)^{-1}\mathbf{K}_s \\ \mathbf{I} & \mathbf{0} \end{bmatrix} \tag{5.7}$$

and

$$\mathbf{B}_m = \begin{bmatrix} (\mathbf{M}_s + \Delta\mathbf{M}_s)^{-1}\mathbf{U} \\ \mathbf{0} \end{bmatrix}. \tag{5.8}$$

The joint system and control equations of motion are now

$$\dot{\bar{\mathbf{x}}}(t) = \bar{\mathbf{A}}_m \bar{\mathbf{x}}(t) \tag{5.9}$$

where

$$\bar{\mathbf{A}}_m = \begin{bmatrix} \mathbf{A}_m - \mathbf{B}_m\mathbf{F} & \mathbf{B}_m\mathbf{F} \\ \mathbf{0} & \mathbf{A}_m - \mathbf{KC} \end{bmatrix} \tag{5.10}$$

The quadratic performance index Eq. (3.14) is evaluated for different locations of the lumped mass on the vertical beam and for six mode shapes as initial conditions. The added mass is 1% of the total mass of the structure. For the case when the mass is located at the bottom of the beam and the fifth mode shape is used as the initial condition the performance index changed from 77.92 to 87.48 or by 12.2%. Results for other locations of the lumped mass and initial conditions are similar, and those with higher percentage changes in the quadratic performance index are shown in Table 23.

The second alternative is a Fixed Model (FM) approach where the observer works in the absence of information about the structural change (See control system block diagram on Fig. 12b.). This case represents changes or errors in the structural model which are not known. The $\bar{\mathbf{A}}_m$ matrix in the joint equation of motion is now:

$$\bar{\mathbf{A}}_m = \begin{bmatrix} \mathbf{A}_m - \mathbf{B}_m\mathbf{F} & \mathbf{B}_m\mathbf{F} \\ \Delta\mathbf{A} - \Delta\mathbf{BF} & \mathbf{A} + \Delta\mathbf{BF} - \mathbf{KC} \end{bmatrix} \tag{5.11}$$

Results of change in performance index are given in Table 23. The change in the system performance for the FM alternative are generally smaller than for the UM

alternative. For instance, 5.8% change for 1% mass added at grid point 9 and fifth mode initial condition compared with 12.2% for UM. We thus get the intriguing result that the LQG design is more robust if changes in the structure are not accounted for in the filter model.

5.6 Comparison of the CDRF and LQG Control Stability Sensitivity due to Structural Changes and Model Reduction

The stability sensitivity of the LQG fixed model to model reduction and comparison with two CDRF control techniques is performed. The changes in the structure are represented with a lumped mass located at one of the model grid points. The LQG reduced model system matrix is now

$$\mathbf{A}_{mE} = \begin{bmatrix} \mathbf{A}_m & -\mathbf{B}_m\mathbf{F}_R \\ \mathbf{K}_R\mathbf{C} & \mathbf{A}_R - \mathbf{K}_R\mathbf{C}_R - \mathbf{B}_R\mathbf{F}_R \end{bmatrix} \tag{5.12}$$

A new form of the joint equation of motion , i.e. Eq. (5.17), is required here because of the reduced-model design of controller (see Eq. [3.19] for unmodified structure). It is found that adding 1% of the total structural mass at the bottom of the beam would cause 54% shift of the pole of the eighth residual mode toward the unstable region. See Table 24 and columns for 1% added mass of three controls. This table shows the most critical cases of stability loss for the respective masses. The same addition of the mass would cause 28% positive shift of the

eighteenth system mode for both MF-DRF and LQ-DRF control design. Therefore, higher percentage in one of the pole's movement of the LQG reduced design will further worsen system stability and one could expect that at some point of structural modification the system will loose its stability completely. Indeed, if 10% of the total structural mass is added to grid point 8 it would cause fourth residual mode to lose stability causing the spillover instability (see 10% added mass columns in Table 24).

Table 9. Change in damping ratios for three critical modes due to a concentrated mass equal to 1% of mass of the structure

Location of Mass, Grid Pt. No.	Change in in Fourth Damping Ratio	Change in in Fifth Damping Ratio	Change in in Sixth Damping Ratio
1	-0.0100	-0.0090	0.0018
2	-0.0033	0.0002	-0.0003
3	0.0000	-0.0009	0.0014
4	-0.0021	-0.0004	-0.0004
5	-0.0055	0.0003	-0.0020
6	-0.0044	-0.0003	-0.0005
7	-0.0007	0.0007	-0.0002
8	0.0016	0.0000	0.0001
9	0.0026	-0.0029	-0.0015

Table 10. Sensitivity of the minimum sum of control gains with respect to 1% added mass for the baseline design * (lb-s/in)

Location of Mass, Grid Pt. No.	$\Delta(\Sigma d_{ii})^{opt}$
1	0.02395
2	0.00745
3	0.00124
4	0.00585
5	0.01347
6	0.01141
7	-0.00011
8	-0.00402
9	0.00285

* Σd_{ii} = 0.10324 (lb-s/in)

Table 11. The comparison between sensitivity analysis prediction results and reoptimization for 0.86% added mass (at grid point 1) design (lb-s/in)

Gain	Sensitivity Analysis from Eq. (3.45)	by Reoptimization
d_{11}	0.05735	0.05779
d_{22}	0.04992	0.05185
d_{33}	0.01663	0.01595
Σd_{ii}	0.12390	0.12559

Table 12. Sensitivity derivatives of the sum of control gains with respect to the beam element thickness for the baseline design

Element	Sensitivity Derivative ($lb\text{-}s/in^2$)
I	0.869
II	0.059
III	-0.065
IV	0.218
V	0.098
VI	0.404
VII	0.393
VIII	0.009

Table 13. Sensitivity derivatives of the second controller gain with respect to the beam element thickness for the baseline design

Element	$\partial d_{22}^{ggt}/\partial t_k$ (lb-s/in^2)
I	1.565
II	0.075
III	-0.280
IV	-0.106
V	-0.498
VI	0.707
VII	0.832
VIII	-0.201

Table 14. Results of re-optimization of control system using control gains and thickness as the design variables and baseline design as starting point

Element	Percentage change of thickness with respect to baseline thickness
I	-10
II	8
III	-10
IV	-10
V	-10
VI	-10
VII	6
VIII	-10

Table 15. Sensitivity of performance to added mass for two control couple UDRF design with constraint on time decay

Location of Mass Grid Pt. No.	Sensitivity (s^{-1}) $\partial f^{opt}/\partial m_k$
1	-23.40
2	-17.60
3	-1.53
4	14.45
5	30.24
6	52.00
7	42.37
8	28.93
9	-28.43

Table 16. Sensitivity of performance index to change in thickness for the UDRF control with constraint on time decay

Element No.	Sensitivity (lb-s/in^2) $\partial f^{opt}/\partial t_k$
I	-0.2771
II	-0.1147
III	0.1462
IV	1.2638
V	1.0917
VI	1.5354
VII	1.7660
VIII	0.1071

Table 17. Final UDRF control design with constraint on time decay

Element No.	New Normalized Thickness
I	0.95
II	0.96
III	0.95
IV	0.95
V	0.95
VI	0.95
VII	0.95
VIII	1.05

Table 18. Theoretical and experimental modal damping ratios for 1.31% added mass design (at grid point 1)

Mode No.	Theory	Experiment
1	0.218	0.187
2	0.043	0.038
3	0.085	0.059
4	0.017	0.020
5	0.029	0.021
6	0.032	0.031

Table 19. Theoretical and experimental modal damping factors

Mode No.	Uniform Gain Design		Baseline Design		2.0% Added Mass (at Grid Pt. 8) Design	
	Theory	Experiment*	Theory	Experiment*	Theory	Experiment*
1	0.074	0.068 (1.3)	0.219	0.200 (6.1)	0.194	0.170 (0.7)
2	0.018	0.017 (6.2)	0.046	0.040 (5.7)	0.047	0.047 (1.4)
3	0.022	0.024 (9.7)	0.071	0.050 (1.1)	0.074	0.062 (7.6)
4	0.010	0.010 (4.6)	0.030	0.036 (13.3)	0.030	0.034 (10.5)
5	0.013	0.013 (6.6)	0.030	0.024 (1.9)	0.030	0.022 (0.7)
6	0.008	0.007 (3.5)	0.030	0.029 (14.0)	0.030	0.028 (5.5)

*The experimental modal damping factor presented is the average of three separate measurements. The value given in parentheses is the percent of the standard deviation of those three measurements relative to the average.

Table 20. Approximate gain matrix D for MF-DRF control (lb-s/in)

Actuator Grid Pt. No.	Sensor Grid Pt. No. 5	7	9
5	0.0508	0.0000	0.0003
7	0.0000	0.0311	-0.0129
9	0.0003	-0.0129	0.0223

Table 21. Sensitivity of performance index with respect to added mass for baseline design

Location of Mass Grid Pt. No.	Sensitivity $(s/in)^2$ $\partial f^{opt}/\partial m_k$
1	21.57
2	11.12
3	-7.84
4	6.59
5	27.94
6	14.61
7	3.35
8	-3.59
9	11.08

Table 22. Change in the fourth damping ratio due to a concentrated mass equal to 1% of mass of the structure for MF-DRF design

Location of Mass Grid Pt. No.	$\Delta\zeta_4$
1	-0.0078
2	-0.0023
3	0.0001
4	-0.0021
5	-0.0046
6	-0.0034
7	-0.0003
8	0.0007
9	-0.0003

Table 23. Percentage change of quadratic performance index due to 1% added mass

Location of Mass Grid Pt. No.	Initial Conditions Mode No.	LQG Full-order Model	
		Updated Model	Fixed Model
1	2	1.0	2.5
1	4	5.6	2.9
1	5	-3.1	1.7
1	6	-2.8	-1.8
2	2	0.8	1.7
3	5	1.6	1.5
4	4	2.3	1.4
5	1	0.9	0.6
5	2	-2.0	-0.6
5	4	2.6	2.6
6	4	3.1	2.3
8	3	4.2	0.7
9	5	12.2	5.8
9	6	8.6	4.2

Table 24. Pole move percentage toward unstable region for three control designs and 1% and 10% added mass

Location of Mass Grid Pt. No.	LQG-FM Design		MF-DRF Design		LQ-DRF Design	
	1%*	10%*	1%*	10%*	1%*	10%*
1	small		22 (4)	46	13	21
2	11 (15**)	39	17 (15)	47	12	33
3	small		16 (9)	49	9	37
4	12 (15)	38	17 (15)	50	13	40
5	15 (16)	59	16 (10)	72	13	61
6	small		11 (4)	59	7	43
7	11 (14)	78	small			
8	40 (14)	spill	small			
9	54 (18)	48	28 (18)	77	28	79

* Percent of total mass added
** Closed-loop mode for which pole move occurred
Small - percent change is less than 10%
Spill - spillover occurred

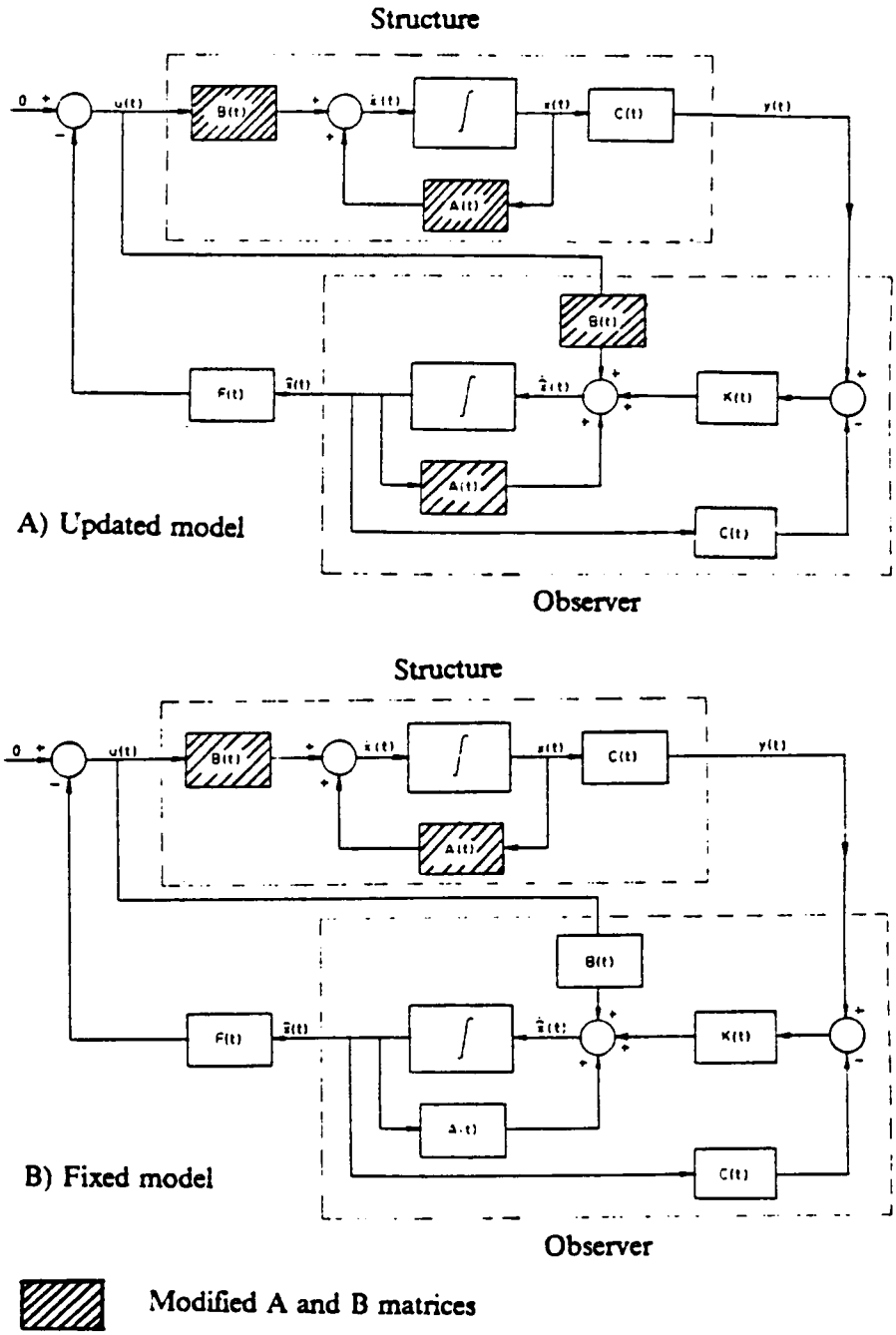

Figure 12. Control system block diagram for Updated Model and Fixed Model

Chapter 6

Summary and Conclusions

The analytical study presented here was motivated by two key problems facing designers of active control for vibration suppression in large space structures. The first problem is the robustness of the feedback control system and is related to the sensitivity of the performance and stability of control system to changes in structure and to model reduction. The second problem is the need for integrated structure/control design, and the assessment of that need can be helped by sensitivity analysis of the optimum control design.

Three direct rate feedback control techniques were studied on the structural model which had similar characteristics to a LSS and then compared to standard LQG control. The baseline design of each control system was obtained first, and after that sensitivity analysis was conducted.

The simplistic uncoupled DRF control law which minimized sum of gains subject to requirements on performance of the system was not robust to structural

changes. However, some small changes in the structure caused a notable increase in performance compared to that of the baseline design and therefore indicated potential for simultaneous structure/control design.

Two coupled DRF techniques were proposed and compared with standard LQG control. The Minimum Force DRF law minimized maximum force of any actuator, while the Linear Quadratic DRF law minimized the standard quadratic performance index for initial conditions in the shape of the first six natural modes. Both techniques guaranteed system stability.

Results for the baseline design showed that LQ-DRF law minimized control effort with system response bounded by the required stability margin. The MF-DRF optimum design was not sensitive to changes in the structure, and therefore the synergistic effect was not significant for this control law. The performance analysis using the same quadratic performance index for evaluation showed that the LQG design was marginally better than the MF-DRF design and poorer than the LQ-DRF design. However the two DRF control laws which do not require model reduction while the LQG control required it and exhibited spillover instability when a lumped mass was added to the structure.

A separate experimental study was conducted simultaneously with this study to verify theoretical results. Good agreement was found between analytical results and experimental measurements for the investigated control techniques.

Better robustness to structural changes, no need for model reduction, and simpler experimental implementation of coupled DRF control together with

comparable or better performance favored these techniques in this study over the model reduction sensitive LQG technique.

References

[1] Balas, M. J., "Trends in Large Space Structures Control Theory: Fondest Hopes, Wildest Dreams", IEEE Trans. Aut. Cont. AC-27, No. 3, June 1982, pp. 522-535.

[2] Andersen, G. C., Garrett, L. B., and Calleson, R. E., "Comparative Analysis of On-orbit Dynamic Performance of Several Large Antenna Concepts", The AIAA/ASME/ASCE/AHS 26th Structures, Structural Dynamics and Materials Conference, AIAA Paper No. 85-0818, Orlando, Florida, April , 1985.

[3] Meirovitch, L., "Computational Methods in Structural Dynamics", Sijthoff and Noordhoff, The Netherlands, 1980.

[4] Athanas, M., "The Role and Use of the Stochastic Linear-Quadratic-Gaussian Problem in Control System Design", IEEE Transactions on Automatic Control, Vol. AC-16, No. 6, December 1971, pp. 529-552.

[5] Balas, M. J., "Active Control of Flexible Systems", Journal of Optimization Theory and Aplications, Vol. 25, No. 3, July 1978, pp. 415-436.

[6] McLaren, M. D., and Slater, G. L., "Robust Multivariable Control of Large Space Structures Using Positivity", AIAAA Paper 86-2125-CP presented at the AIAA Astrodynamics Conference, Williamsburg,Va, August 1986.

[7] Santiago, J. M., Lange W. J., Jr., and Jamshidi, M., "An Overview of Latest Model Reduction and Control Methods of Large Flexible Space Structures",

Proceedings of the Workshop on Indentification and Control of Flexible Space Structures, G. Rodriguez (Ed.), JPL Publication 85-29, Vol. II, pp. 381-395, April 1, 1985.

[8] Steiber, M. E., "Design and Evaluation of Control Systems for Large Communications Satellites", Proceedings of the Workshop on Indentification and Control of Flexible Space Structures, G. Rodriguez (Ed.), JPL Publication 85-29, Vol. I, pp. 183-197, April 1, 1985.

[9] Skidmore, G. R., and Hallauer W. L. Jr., "Experimental-Theoretical Study of Active Damping With Dual Sensors and Actuators," AIAA Paper No. 85-1921-CP, AIAA Guidance, Navigation, and Control Conference, Snowmass, Colorado, August 19-21, 1985, pp. 433-442 in AIAA CP856.

[10] Skidmore, G. R., and Hallauer W. L. Jr., "Modal-Space Active Damping of a Beam-Cable Structure: Theory and Experiment", Journal of Sound and Vibration , 1985, 101(2), pp. 149-160.

[11] Dehghanyar, T. J., Masri, S. F., Miller, R. K., and Bekey, G. A., "Suboptimal Control of Nonlinear Flexible Space Structures", Proceedings of the Workshop on Indentification and Control of Flexible Space Structures, G. Rodriguez (Ed.), JPL Publication 85-29, Vol. II, pp. 365-380, April 1, 1985.

[12] Horner, G. C,"Optimum Actuator Placement, Gain, and Number for a Two-dimensional Grillage," AIAA paper No. 83-0854 presented at the AIAA/ASME/ASCE/AHS 24th Structures, Structural Dynamics, and Materials Conference, Lake Tahoe, Nevada, May 2-4, 1983.

[13] Horner, G. C., and Walz, J. E., "A Design Technique for Determining Actuator Gains in Spacecraft Vibration Control", The AIAA/ASME/ASCE/AHS 26th Structures, Structural Dynamics and Materials Conference, AIAA Paper No. 85-0628, Orlando, Florida, April , 1985.

[14] Balas, M. J., "Direct Output Feedback Control of Large Space Structures", The Journal of Astronautical Sciences, Vol. XXVII, No. 2. pp. 157-180, April-June, 1979.

[15] Balas, M. J., "Direct Velocity Feedback Control of Large Space Structures", Journal of Guidance and Control, Vol. 2, No. 3, 1983, pp. 252-253.

[16] Manning, R. A., Lust, R. V., and Schmit, L. A., "Behavior Sensitivities for Control Augmented Structures", Sensitivity Analysis in Engineering, NASA Conference Publication 2457, Proceedings of a symposium held at Langley Research Center, Hampton, Virginia, September 25-26, 1986, pp. 33-57.

[17] Canavin, J.R., "The Control of Spacecraft Vibrations Using Multivariable Output Feedback," AIAA Paper 78-1419, AIAA/AAS Astrodynamics Conference, Palo Alto, California, August 7-9, 1978.

[18] Elliott, L.E., Mingori, D.L., and Iwens, R.P., "Performance of Robust Output Feedback Controller for Flexible Spacecraft," Dynamics and Control of Large Flexible Spacecraft, Proceedings of the Second VPI&SU/AIAA Symposium, 1979, pp. 409-420.

[19] Martinovic, Z. N., Haftka, R. T., Hallauer, W. L., and Schamel, G. C. II, "A Comparison of Active Vibration Control Techniques: Output Feeedback vs. Optimal Control," AIAA Dynamics Specialists Conference, Monterey, California, April 9-10, 1987, AIAA Paper No. 87-0904-CP, pp. 610-621 in Part 2B of AIAA CP873.

[20] Martinovic, Z. N., Schamel, G. C. II,Haftka, R. T., and Hallauer, W. L., "An Analytical and Experimental Investigation of Output Feedback vs. Linear Quadratic Regulator," AIAA Guidance, Navigation, and Control Conference, Monterey, California, August 17-19, 1987, AIAA Paper No. 87-2190-CP.

[21] Hale, A. L., "Integrated Structural/Control Synthesis via Set-Theoretic Methods" The AIAA/ASME/ASCE/AHS 26th Structures, Structural Dynamics and Materials Conference, AIAA Paper No. 85-0806, Orlando, Florida, April , 1985.

[22] Hoehne, V. O., "AFWAL Control Technology Programs", Proceedings of the Workshop on Indentification and Control of Flexible Space Structures, G. Rodriguez (Ed.), JPL Publication 85-29, Vol. I, pp. 13-31, April 1, 1985.

[23] Kosut, R. L., Salzwedel, H., and Naeini, A. E., "Robust Control of Flexible Spacecraft", Journal of Guidance, Control and Dynamics, Vol. 6, No. 2, March-April, 1983, pp. 104-111.

[24] Yedavalli, R. K., Banda, S. S., and Ridgley, D. B., "Time-Domain Stability Robustness Measures for Linear Regulators", Journal of Guidance, Control and Dynamics, Vol. 8, No. 4, July-August, 1985, pp. 520-524.

[25] Hamer, H. A., and Johnson K. G., "Effects of Model Error on Control of Large Flexible Space Antenna With Comparisons of Decoupled and Linear Quadratic Regulator Control Procedures", NASA Technical Paper 2604, September 1986.

[26] Schaechter, D. B., "Closed-Loop Control Performance Sensitivity to Parameter Variations", Journal of Guidance, Control and Dynamics, Vol. 6, No. 5, Sept-Octob., 1983, pp. 399-402.

[27] Gilbert, M. G., "Design Paramter Sensitivity Methods in Optimal LQG Control Law Synthesis", AIAA Paper No. 85-1930-CP, AIAA Guidance, Navigation, and Control Conference, Snowmass, Colorado, August 19-21, 1985.

[28] Gilbert, M. G., "Sensitivity Method for Integrated Structure/Active Control Law Design", Sensitivity Analysis in Engineering, NASA Conference Publication 2457, Proceedings of a symposium held at Langley Research Center, Hampton, Virginia, September 25-26, 1986, pp. 59-75.

[29] Junkins, J. L., and Rew, D. W., "Unified Optimization of Structures and Controllers", Large Space Structures: Dynamics and Control, Editors S. N. Alturi and A. K. Amos, Springer-Verlag, Berlin, Heidelberg, New York, Tokio, to appear 1987.

[30] Eastman, W. L., and Bossi, J. A., "Robust Control Design for Large Space Structures", Proceedings of the Workshop on Indentification and Control of Flexible Space Structures, G. Rodriguez (Ed.), JPL Publication 85-29, Vol. III, pp. 63-82, April 1, 1985.

[31] Meirovitch, L., and Norris M. A., "Sensitivity of Distributed Structures to Model Order in Feedback Control", The AIAA Dynamics Specialists Conference, AIAA Paper No. 87-0900, Monterey, California, April 9-10, 1987.

[32] Joshi, S. M., "Control Systems Synthesis for a Large Flexible Space Antenna," Acta Astronautica, Vol. 10, No. 5-6, 1983, pp. 365-380.

[33] Joshi, S. M., "Robustness Properties of Collocated Controllers for Flexible Spacecraft," Journal of Guidance, Control, and Dynamics, Vol. 9, No. 1, January-February, 1986, pp. 85-91.

[34] Meirovitch, L., and Baruh, H., "Robustness of the Independent Modal-Space Control Method", Journal of Guidance, Control and Dynamics, Vol. 6, No. 1, Jan.-Feb., 1983, pp. 20-25.

[35] Hale, A. L., Lisowski, R. J., and Dahl, W. L., "Optimal Simultaneous Structural and Contol Design of Maneuvering Flexible Spacecraft", Journal of Guidance, Control and Dynamics, Vol. 8, No. 1, Jan.-Feb., 1985, pp. 86-93.

[36] Salama, M., Hamidi, M. and Demsetz, L., "Optimization of Controlled Structures", Proceedings of the Workshop on Indentification and Control of Flexible Space Structures, G. Rodriguez (Ed.), JPL Publication 85-29, Vol. II, pp. 311-327, April 1, 1985.

[37] Hanks, B. R., and Skelton, R. E., "Designing Structures for Reduced Response by Modern Control Theory", The AIAA/ASME/ASCE/AHS/ 24th

Structures, Structural Dynamics, and Materials Conference, AIAA Paper No. 83-0815, Lake Tahoe, Nevada, May 2-4, 1983.

[38] Onoda, J., and Haftka, R. T., "Simultaneous Structure/Control Optimizaion for Large Flexible Spacecraft", The AIAA/ASME/ASCE/AHS 28th Structures, Structural Dynamics and Materials Conference, AIAA Paper No. 87-0823, Monterey, California, April 6-8, 1987.

[39] Mesaac, A., Turner, J., and Soosaar, K., "An Integrated Control and Minimum Mass Structural Optimization Algorithm for Large Space Strucures", Proceedings of the Workshop on Indentification and Control of Flexible Space Structures, G. Rodriguez (Ed.), JPL Publication 85-29, Vol. II, pp. 231-256, April 1, 1985.

[40] Gustafson, C. L., Aswani, M., Doran, A. L., and Tseng, G. T., "ISAAC (Integrated Structural Analysis and Control) via Continuum Modeling and Distributed Frequency Domain Design Techniques", Proceedings of the Workshop on Indentification and Control of Flexible Space Structures, G. Rodriguez (Ed.), JPL Publication 85-29, Vol. II, pp. 287-310, April 1, 1985.

[41] Khot, N. S., Grandhi R. V., and Venkayya V. B., "Structural and Control Optimization of Space Structures", The AIAA Dynamics Specialists Conference, AIAA Paper No. 87-0939, Monterey, California, April 9-10, 1987.

[42] Bendsoe, M. P., "Design of Structure and Controllers for Optimal Performance", NATO ASI Series Vol. F27 Computer Aided Optimal Design: Structural and Mechanical Systems, Edited by C. A. Mota Soares, Springer-Verlag, Berlin, Heidelberg, 1987. pp. 181-193.

[43] Khot, N. S., "Minimum Weight and Optimal Control Design of Space Strustures", NATO ASI Series Vol. F27 Computer Aided Optimal Design: Structural and Mechanical Systems, Edited by C. A. Mota Soares, Springer-Verlag, Berlin, Heidelberg, 1987. pp. 389-403.

[44] Haftka, R. T., "Optimum Control of Structures", NATO ASI Series Vol. F27 Computer Aided Optimal Design: Structural and Mechanical Systems, Edited by C. A. Mota Soares, Springer-Verlag, Berlin, Heidelberg, 1987. pp. 381-388.

[45] Khot, N. S., Eastep, F. E., and Venkayya, V. B., "Optimal Structural Modifications to Enhance the Optimal Active Vibration Control of Large Flexible Structures", The AIAA/ASME/ASCE/AHS 26th Structures, Structural Dynamics and Materials Conference, AIAA Paper No. 85-0627, Orlando, Florida, April , 1985.

[46] Khot, N. S., Eastep, F. E., Oz, H., and Venkayya, V. B., "Optimal Structural Design to Modify the Vibration Control Gain Norm of Flexible Structures", The

AIAA/ASME/ASCE/AHS 27th Structures, Structural Dynamics and Materials Conference, AIAA Paper No. 86-0842, San Antonio, California, 1986.

[47] Haftka, R.T., Martinovic, Z.N., and Hallauer, W.L.,Jr., "Enhanced Vibration Controllability by Minor Structural Modification," AIAA Journal, Vol. 23, Aug. 1985, pp 1260-1266.

[48] Haftka, R.T., Martinovic, Z.N., and Hallauer, W.L.,Jr., and Schamel, G., "An Analytical and Experimental Study of a Control System's Sensitivity to Structural Modifications," AIAA Journal, Vol. 25, Feb. 1987, pp 310-315.

[49] Haftka, R.T., and Kamat, M.P., "Elements of Structural Optimization", Martinus Nijhoff, The Netherlands, 1985, pp. 181-183.

[50] Hallauer, W. L., and Barthelemy, J. F. M., "Active Damping of Modal Vibrations by Force Apportioning", AIAA Paper No. 80-0806, AIAA/ASME/ASCE/AHS 21st Structures, Structural Dynamics & Materials Conference, May 12-14, 1980, Seatle, Washington.

[51] Kwakernaak, H., and Sivan, R., "Linear Optimal Control Systems", Wiley, 1972.

[52] Anderson, B.D.O., and Moore, J.B.,"Linear Optimal Control", Prentice-Hall,Inc., 1971. p. 50.

[53] Kammer, D. C., and Sesak, J. R., "Actuator Number Versus Parameter Sensitivity in Flexible Spacecraft Control", Second VPI & SU/AIAA Symposium on Dynamics and Control of Large Flexible Spacecraft, Blacksburg, Va., 1979.

[54] Thareja, R., and Haftka, R.T., "NEWSUMT-A, A General Purpose Program for Constrained Optimization Using Constraint Approximations," ASME Journal of Mechanics, Transmission, and Automation in Design, March 1985, pp. 94-99.

[55] Schamel, G. C. II, "Active Damping of a Structure with Low Frequency and Closely Spaced Modes: Experiments and Theory," M.S. Thesis,VPI&SU, Blacksburg, VA, March 1985.

Appendix A

Model Reduction

Given the full-order model ($n_n x n_n$) of a system

$$\mathbf{M}_s\ddot{\mathbf{q}}(t) + \mathbf{K}_s\mathbf{q}(t) = \mathbf{0} \qquad (A.1)$$

we can find an n_n order modal matrix $\mathbf{\Phi}$, natural frequency matrix $diag(\omega_i^2)$ and the modal mass matrix $diag(\mathrm{M}_i)$.

Next, we select n_R degrees of freedom and number of modes that we wish to retain in the reduced order model. Reordering the modal matrix and partitioning it

$$\mathbf{\Phi} = \begin{bmatrix} \mathbf{\Phi}_{R\,(n_R x n_R)} & \mathbf{\Phi}_{12\,(n_R x [n_n - n_R])} \\ \mathbf{\Phi}_{21\,([n_n - n_R] x n_R)} & \mathbf{\Phi}_{22\,([n_n - n_R] x [n_n - n_R])} \end{bmatrix} \qquad (A.2)$$

We use only the reduced modal matrix Φ_R and corresponding reduced frequency and modal mass matrices

$$diag(\omega_i^2) = diag(\omega_1^2, ..., \omega_{n_R}^2)$$

$$diag(M_i) = diag(M_1, ..., M_{n_R})$$

and define reduced physical damping, stiffness, and mass matrices respectively as

$$\mathbf{C}_{sR} = \Phi_R^{-T} [diag(2\zeta_i \omega_i M_i)]_R \Phi_R^{-1} \tag{A.3}$$

$$\mathbf{K}_{sR} = \Phi_R^{-T} [diag(\omega_i^2 M_i)]_R \Phi_R^{-1} \tag{A.4}$$

$$\mathbf{M}_{sR} = \Phi_R^{-T} [diag(M_i)]_R \Phi_R^{-1} \tag{A.5}$$

Premultiplying Eqs. (A.3)-(A.4) by the inverted reduced modal mass matrix, and postmultiplying inverted reduced modal mass matrix with reduced applied load distribution matrix $\mathbf{U}_{sR}$, we obtain the following matrices required in the reduced state space equations of the system:

$$\mathbf{M}_{sR}^{-1}\mathbf{C}_{sR} = \Phi_R [diag(2\zeta_i \omega_i)]_R \Phi_R^{-1} \tag{A.6}$$

$$\mathbf{M}_{sR}^{-1}\mathbf{K}_{sR} = \Phi_R [diag(\omega_i^2)]_R \Phi_R^{-1} \tag{A.7}$$

$$\mathbf{M}_{sR}^{-1}\mathbf{U}_{sR} = \Phi_R [diag(M_i^{-1})]_R \Phi_R^T \mathbf{U}_{sR} \tag{A.8}$$

Appendix B

The Alpha-shifted Performance Index

The exponentionally weighted quadratic performance index is one way to achieve a control law that gives not merely an asymptotically stable closed-loop system, but one with a degree of stability at least some prescribed value α. The alpha-shift theory is presented here (based on [52]) for the regulator problem but it may be implemented in the observer design due to duality between the regulator and the observer.

Given the system

$$\dot{\mathbf{x}}(t) = \mathbf{A}\,\mathbf{x}(t) + \mathbf{B}\,\mathbf{u}(t) \qquad (B.1)$$

and control

$$\mathbf{u}(t) = -\mathbf{F}\mathbf{x}(t). \qquad (B.2)$$

the exponentially weighted performance index has the form

$$J = \int_0^\infty e^{2\alpha t}[\mathbf{x}(t)^T\mathbf{Q}\mathbf{x}(t) + \mathbf{u}(t)^T\mathbf{R}\mathbf{u}(t)]dt \qquad (B.3)$$

This problem can be converted to a 'standard' one by introducing the transformation

$$\bar{\mathbf{x}}(t) = e^{\alpha t}\mathbf{x}(t) \qquad (B.4)$$

$$\bar{\mathbf{u}}(t) = e^{\alpha t}\mathbf{u}(t) \qquad (B.5)$$

Differentiating Eq. (B.4) with respect to time and using Eq. (B.1) one can reach the transformed sytem equation

$$\dot{\bar{\mathbf{x}}}(t) = (\mathbf{A} + \alpha\mathbf{I})\,\bar{\mathbf{x}}(t) + \mathbf{B}\,\bar{\mathbf{u}}(t) \qquad (B.6)$$

and introducing transformation Eqs. (B.4)-(B.5) into integral of Eq. (B.3), a standard form of quadratic performance index is obtained

$$J = \int_0^\infty [\bar{\mathbf{x}}(t)^T\mathbf{Q}\bar{\mathbf{x}}(t) + \bar{\mathbf{u}}(t)^T\mathbf{R}\bar{\mathbf{u}}(t)]dt \qquad (B.7)$$

The requirement that $\mathbf{x}(t)$ will decay faster than $e^{-\alpha t}$ is equivalent to requiring that $\bar{\mathbf{x}}$ is stable. The solution of the transformed problem is obtained by solving Riccati equation:

$$(\mathbf{A} + \alpha\mathbf{I})^T\mathbf{S}_r + \mathbf{S}_r(\mathbf{A} + \alpha\mathbf{I}) - \mathbf{S}_r\mathbf{B}\,\mathbf{R}^{-1}\mathbf{B}^T\mathbf{S}_r + \mathbf{Q} = \mathbf{0}, \qquad (B.8)$$

For relatively large values of α the stability margin becomes close to -2α. This can easily be shown for a single DOF system. The original system is described by

$$\dot{x}(t) = ax(t) + u \tag{B.9}$$

and the control as

$$u(t) = -fx(t) = -sx(t) \tag{B.10}$$

The performance index is

$$J = \int_0^\infty e^{2\alpha t}(qx^2 + u^2)dt \tag{B.11}$$

The transformed problem is

$$\dot{\bar{x}}(t) = (a + \alpha)\bar{x}(t) + \bar{u} \tag{B.12}$$

$$J = \int_0^\infty (q\bar{x}^2 + \bar{u}^2)dt \tag{B.13}$$

Riccati equation for this system is

$$(a + \alpha)s + s(a + \alpha) - s^2 + q = 0 \tag{B.14}$$

The positive root of this equation is

$$s = (a + \alpha) + \sqrt{(a + \alpha)^2 + q} \tag{B.15}$$

Original closed-loop system is

$$\dot{x}(t) = (a - s)x(t) \qquad (B.16)$$

and its single root is equal to $\alpha + \sqrt{(a + \alpha)^2 + q}$. For large values of α this root approaches 2α.

Appendix C

Minimum Euclidian Norm

The optimum design problem for the Minimum Euclidian Norm [46] control cases is formulated as

$$\text{find} \quad \mathbf{D} \tag{C.1}$$

$$\text{to minimize } f(\mathbf{D}) = ||\mathbf{D}|| = \left(\sum_{i=1}^{n_c}\sum_{j=1}^{n_c} d_{ij}^2\right)^{1/2}$$

$$\text{subject to } g_j = \zeta_j - \zeta_L \geq 0 \quad j = 1,\ldots, n_m$$

$$\text{and } \mathbf{D} > 0 \quad i = 1,\ldots, n_c$$

Appendix D

Performance Index

For the determination of the performance indices, all the system equations will be represented in the following form

$$\dot{\mathbf{x}}(t) = \mathbf{A}\,\mathbf{x}(t) \tag{D.1}$$

with the initial state $x(t_0)$. For the solution of this equation we write

$$x(t) = \Phi(t, t_0)x(t_0) \tag{D.2}$$

where

$$\Phi(t, t_0) = e^{\mathbf{A}(t - t_0)} \tag{D.3}$$

is the transition matrix of the time-invariant system Eq. C.1.

The performance index that represents some quadratic measure of the state $\mathbf{x}$ in time can expressed as

$$J = \int_{t_0}^{\infty} \mathbf{x}(t)^T \mathbf{Q} \mathbf{x}(t) dt \qquad (D.4)$$

This performance index becomes equal [51] to

$$J = \mathbf{x}(t_0)^T \mathbf{P}\, \mathbf{x}(t_0) \qquad (D.4)$$

where for $t_0 = 0$

$$\mathbf{P} = \int_0^{\infty} e^{\mathbf{A}^T t} \mathbf{Q} e^{\mathbf{A}t} dt \qquad (D.5)$$

satisfying Lyapunov matrix equation

$$\mathbf{A}^T \mathbf{P} + \mathbf{P}\mathbf{A} + \mathbf{Q} = \mathbf{0} \qquad (D.5)$$

The vita has been removed from the scanned document